

**DYNAMIC LOAD ANALYSIS OF THE MICRO
UNMANNED AERIAL VEHICLE (UAV) STRUCTURE**

MOHAMAD IZHAM BIN MOHAMAD ZAINAL

**MECHANICAL ENGINEERING
UNIVERSITI TEKNOLOGI PETRONAS
JUNE 2010**

CERTIFICATION OF APPROVAL

**Dynamic Load Analysis of the Micro Unmanned Aerial Vehicle (UAV)
Structure**

by

Mohamad Izham Bin Mohamad Zainal

A project dissertation submitted to the
Mechanical Engineering Programme
Universiti Teknologi PETRONAS
in partial fulfilment of the requirement for the
BACHELOR OF ENGINEERING (Hons)
(MECHANICAL ENGINEERING)

Approved by,

(IR IDRIS BIN IBRAHIM)

UNIVERSITI TEKNOLOGI PETRONAS

TRONOH, PERAK

JUNE 2010

CERTIFICATION OF ORIGINALITY

This is to certify that I am responsible for the work submitted in this project, that the original work is my own except as specified in the references and acknowledgements, and that the original work contained herein have not been undertaken or done by unspecified sources or persons.

MOHAMAD IZHAM BIN MOHAMAD ZAINAL

ABSTRACT

Unmanned Aerial Vehicle (UAV) is unpiloted aircraft that can be remote controlled or fly autonomously based on pre-programmed flight plans or more complex dynamic automation systems. One of the critical parts in developing an UAV is the structural dynamic analysis on the structure itself. This project is undertaken with specific objective which is to do dynamic analysis onto the designed micro UAV structure.

During the progress to complete the project, information gathered from all reliable sources including the properties of the materials involved, the suitable method in producing the dynamic analysis, and others. After the reviews of the literature being completed, the project methodology will be developed. In the methodology, the best suitable method will be implemented to do the analysis, and in this case, Newtonian method was chosen. In this project, Acrylonitrile butadiene styrene (ABS) had been considered to be the structure material. For the first step in project methodology, mathematical modelling will be developed. Using data and sources gathered, then, analysis will be done to determine the structure's mode shapes and response. After the calculation was completed, the results gained will then being compared and validated by referring to the existed journals and articles about the structural dynamics.

Based on the analytical method, the designed structure was achieved to sustain such wind load applied on it by the fans. Referring to the analysis done, the main objectives of this project were achieved. As to enhance more of the analysis and the research study, other method such as Hamilton Principle, Rayleigh method and Finite Element method should be used in the methodology stage, and perhaps, they will give better results and more precise analysis in the project development.

ACKNOWLEDGEMENT

The author wishes to take the opportunity to express his utmost gratitude to the individual that have taken the time and effort to assist the author in completing the project. Without the cooperation of these individuals, no doubt the author would have faced some minor complications through out the course.

First and foremost the author's utmost gratitude goes to the author's supervisor, Mr Ir. Idris Ibrahim. Without his guidance and patience, the author would not be succeeded to complete the project. During the progress of this project, Ir. Idris had provided lots of guidance and advice that is related to the project as well as provided his valuable experience on the field.

To all the students under UAV development which is under the same supervisor, thanks a lot for your cooperation and kindness in assisting the author to complete his project. To all individuals that has helped the author in any way, but whose name is not mentioned here, the author thank you all.

TABLE OF CONTENT

CHAPTER 1 INTRODUCTION	1
1.1 Background	1
1.2 Problem Statement	2
1.3 Objectives and Scope of Study	2
1.4 Relevancy of the project.....	2
1.5 Feasibility of the Project Within the Scope and Time Frame	3
CHAPTER 2 LITERATURE REVIEW.....	4
2.1 Review / Theory	4
2.2 Vibration System.....	4
2.3 Stiffness Analysis.....	6
2.4 Natural and Fundamental Frequency	7
2.5 Mode Shape.....	8
2.6 Dynamic Analysis	9
2.7 Micro Unmanned Aerial Vehicle (UAV) Design	11
CHAPTER 3 METHODOLOGY	14
3.1 Project Flowchart	14
3.2 Project Methodology Sequences	15
3.3 Tools / Equipments Required.....	16
3.4 Materials Properties	16
3.5 Micro Unmanned Aerial Vehicle (UAV) Structure.....	17
3.5.1 Upper Beam	18
3.5.2 Lower Beam	20
3.6 Dynamic Analysis (Force Transfer Through Out The Beams).....	23
3.6.1 Deriving the Equation of Motion	23
3.6.2 Total Response Equation.....	25
3.7 Boundary Condition	28
3.7.1 Lower Beam	28
3.7.2 Upper Beam	30
CHAPTER 4 RESULT AND DISCUSSION	34

4.1	Mode Shapes and Total Response for Lower Beam	34
4.2	Mode Shapes and Total Response for Upper Beam.....	39
4.3	Discussion	42
CHAPTER 5 CONCLUSION AND RECOMMENDATION		47
5.1	Conclusion	47
5.2	Recommendation.....	48
REFERENCES		49
APPENDICES		50
	APPENDIX A Slopes and Deflection of Beams	51
	APPENDIX B Gantt Chart FYP I	52
	APPENDIX C Gantt Chart FYP II	53

LIST OF FIGURES

Figure 2.1: Mass-spring model	5
Figure 2.2: Mass-spring model	6
Figure 2.3: (a) The tall building is simplified as a one-step bar; (b) mass distribution; (c) stiffness distribution.....	10
Figure 2.4: Micro UAV 3D Solid Structure.....	11
Figure 2.5: Micro UAV 3D Wired Structure	12
Figure 3.1: Project Methodology Flowchart	14
Figure 3.2: Micro UAV Structure	17
Figure 3.3: Schematic Diagram of the Upper Beam.....	18
Figure 3.4: Superposition Method for the Upper Beam.....	19
Figure 3.5: Free Body Diagram of the Upper Beam.....	20
Figure 3.6: Schematic Diagram of the Lower Beam.....	20
Figure 3.7: Superposition Method for the Lower Beam	22
Figure 3.8: Free Body Diagram of the Lower Beam	22
Figure 3.9: A Bending Beam	23
Figure 3.10: Lower Beam System with Harmonic Force	25
Figure 3.11: Upper Beam System with Harmonic Force.....	25
Figure 3.12: Lower Beam's Boundary Condition with Harmonic Force.....	28
Figure 3.13: Upper Beam's Boundary Condition with Harmonic Force.....	30
Figure 4.1: Response of the Lower Beam at 5 Hz	36
Figure 4.2: Response of the Lower Beam at 10 Hz	37
Figure 4.3: Response of the Lower Beam at 15 Hz	37
Figure 4.4: Response of the Lower Beam at 20 Hz	38
Figure 4.5: Response of the Lower Beam at 25 Hz	38
Figure 4.6: Response of the Lower Beam at 30 Hz	39
Figure 4.7: Response of the Upper Beam at 5 Hz.....	42
Figure 4.8: Response of the Upper Beam at 10 Hz.....	42
Figure 4.9: Response of the Upper Beam at 15 Hz.....	43
Figure 4.10: Response of the Upper Beam at 20 Hz.....	43
Figure 4.11: Response of the Upper Beam at 25 Hz.....	44
Figure 4.12: Response of the Upper Beam at 30 Hz.....	44

Figure 4.13: Mode Shape and Response of the Fixed End Beam..... 46

LIST OF TABLES

Table 2.1: Design specification of Micro UAV 12

Table 3.1: ABS Properties 17

Table 4.1: Lower Beam's Value of C1, C2, C3 and C4 at 5 Hz..... 34

Table 4.2: Lower Beam's Value of C1, C2, C3 and C4 at 10 Hz..... 34

Table 4.3: Lower Beam's Value of C1, C2, C3 and C4 at 15 Hz..... 35

Table 4.4: Lower Beam's Value of C1, C2, C3 and C4 at 20 Hz..... 35

Table 4.5: Lower Beam's Value of C1, C2, C3 and C4 at 25 Hz..... 35

Table 4.6: Lower Beam's Value of C1, C2, C3 and C4 at 30 Hz..... 36

Table 4.7: Upper Beam's Value of C1, C2, C3 and C4 at 5 Hz 38

Table 4.8: Upper Beam's Value of C1, C2, C3 and C4 at 10 Hz 39

Table 4.9: Upper Beam's Value of C1, C2, C3 and C4 at 15 Hz 39

Table 4.10: Upper Beam's Value of C1, C2, C3 and C4 at 20 Hz 39

Table 4.11: Upper Beam's Value of C1, C2, C3 and C4 at 25 Hz 40

Table 4.12: Upper Beam's Value of C1, C2, C3 and C4 at 30 Hz 40

CHAPTER 1

INTRODUCTION

1.1 Background

An Unmanned Aerial Vehicle (UAV) is a no crewed aircraft. An Unmanned Aerial Vehicle (UAV) is an unpiloted aircraft which can carry cameras, sensors, communications equipment or other payloads. An UAV is defined as a reusable, no crewed vehicle capable of controlled, sustained, level flight and powered by a jet or reciprocating engine. Historically, UAV is a simple drone (remotely piloted aircraft), but autonomous control is increasingly being employed in UAV. UAV comes in two varieties, some are controlled from a remote location, and others fly autonomously based on pre-programmed flight plans using more complex dynamic automation systems.

Most of the UAVs in the world nowadays are built for military purpose. These UAV are used for reconnaissance, surveillance, combat purpose and rescue mission. For this kind of purposes, many military departments around the world had developed the unmanned aircraft technology to carry out the jobs without risking human life or expensive assets. Somehow, the technology becomes more advance and innovative. The UAV produced became smaller and smaller. In order to make UAV more reliable and rigid, some researches were being done and being modelled into Micro Unmanned Aerial Vehicle (MUAV). Basically, micro UAV was invented to perform same purposes with conventional UAV but the different is between the size and capabilities are slightly different.

One of the important components of micro UAV is the structure itself. The structure's design is very important to make sure the micro UAV is safe or not to fly. So, this project is undertaken to perform dynamic analysis onto the micro UAV structure using the design and material decided.

1.2 Problem Statement

For the purpose of this project, the static and dynamic load analysis are very important to assess the structural integrity of the Micro Unmanned Aerial Vehicle (MUAV). The dynamic load due to the wind resistance would make a harmonic motion onto the MUAV movement and its stability. Therefore, it is necessary to carry the static and dynamic load analysis to ensure the MUAV can withstand such both static and dynamic loads during takeoff, floating and landing. However, since there are different conditions of analysis, the result generated is unpredictable. As the result, this project is to create a solution, equation to be precise for the stability of the MUAV structure.

1.3 Objectives and Scope of Study

The objective of this project is to perform dynamic load analysis on the Micro Unmanned Aerial Vehicle structure during static position as well as floating. Further analysis will be carried out by investigating the effect of different materials being used in analysis and also the geometry of the MUAV structure.

1.4 Relevancy of the Project

This project is relevant to Mechanical Engineering academic syllabus of Universiti Teknologi PETRONAS (UTP). It incorporates knowledge in mechanical engineering design, manufacturing technology, engineering materials, dynamics, statics, mechanics of machines, and mechatronics into practical robotics application. In addition, it also enhances project management and communication skills.

1.5 Feasibility of the Project Within the Scope and Time Frame

For this project, the first semester will cover formulation of methodology and documentation of analysis conceptualization. The second semester will be concentrated on detail analysis and simulation of the Micro Unmanned Aerial Vehicle structure during static position as well as floating. Based on the draft methodology, the project's objectives are considered achievable within the given time frame.

CHAPTER 2

LITERATURE REVIEW

2.1 Review / Theory

The research includes, study and analysis with a literature review related to Micro Unmanned Aerial Vehicle (MUAV) structure design data, dynamic analysis and dynamic loading. Perform the dynamic load analysis on the Micro UAV structure design. The load input will be based on the load applied factors. Once the result is acceptable, further investigation will be carried out.

The objective of the present study is to do analysis on vibrations of the component structures significantly influence the motion accuracy and fatigue damage. To analyze the dynamic load of the Micro UAV structure, multi-body dynamic simulation techniques have been used. Various design proposals are investigated to improve structural design performances by using the dynamic simulation model. Design sensitivity analyses with respect to vibration and stresses are carried out to search an optimal design.

Instead of studying the theoretical parts in the references, an analytical study on the journal and papers regarding the dynamic analysis on the structure will be examined in order to see the flow and popular methods to be used in the dynamics research process.

2.2 Vibration System

In this project, basically study about vibration was the first and very important criteria to do whatever analysis of the design structure. Theoretically vibration is

simply the motion of a machine or machine part back and forth from its position of rest. In term of physic, vibration is the response of a system to some internal or external excitation (stimulus) of force applied to the system. Periodically, vibration refers to mechanical oscillations about an equilibrium point [1].

Overall project would be easier in understanding the vibration analysis if compared to the simple mass-spring-damper model. For a whole complex structure such as an automobile body can be modelled as a simple mass-spring-damper model. To start the mathematical modelling, we need to clarify the system is vibration without damping or with damping. For vibration without damping case, we first will assume the damping is negligible and there is no external force applied to the mass (structure) [1].

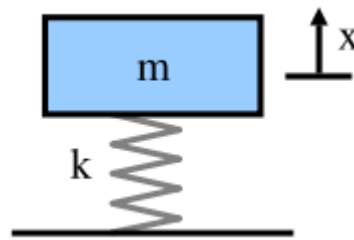


Figure 2.1: Mass-spring model [1]

The force applied to the mass by the spring is proportional to the amount the spring is stretched "x" (we will assume the spring is already compressed due to the weight of the mass). The proportionality constant, k, is the stiffness of the spring and has units of force/distance (e.g. lbf/in or N/m).

$$F_s = -kx \quad \text{Eq. (1)}$$

The force generated by the mass is proportional to the acceleration of the mass as given by Newton's second law of motion.

$$\sum F = ma = m\ddot{x} = m \frac{d^2x}{dt^2} \quad \text{Eq. (2)}$$

Therefore, the sum of the forces on the mass then generates the ordinary differential equation.

$$m\ddot{x} + kx = 0 \quad \text{Eq. (3)}$$

From Equation (3), if we start the system to vibrate by stretching the spring by the distance of 'A' in mode of assumption, the solution that describe the motion of mass is as below.

$$x(t) = A \cos(2\pi f_n t) \quad \text{Eq. (4)}$$

Now in the second condition, we add a viscous damper to the model that outputs a force that is proportional to the velocity of the mass. The proportionality constant c is called the damping coefficient and has units of Force over velocity (lbf s/ in or N s/m).

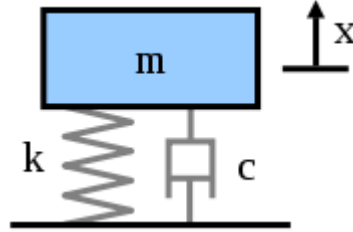


Figure 2.2: Mass-spring model [1]

From Figure (2), the equation is as follow,

$$F_d = -cv = -c\dot{x} = -c \frac{dx}{dt} \quad \text{Eq. (5)}$$

By summing the forces on the mass we get the following ordinary differential equation,

$$m\ddot{x} + c\dot{x} + kx = 0 \quad \text{Eq. (6)}$$

So, from the equation, we can get the solution for the model system,

$$x(t) = X e^{-\zeta \omega_n t} \cos(\sqrt{1 - \zeta^2} \omega_n t - \phi) \quad \text{Eq. (7)}$$

Where,

$$\omega_n = 2\pi f_n \quad \text{Eq. (8)}$$

From the fundamental of vibration that being studied, the problem in dynamic load analysis of the Micro UAV structure can be solved by applying them in the solution. The system also needs to be clarified back whether it is either damping system or not.

2.3 Stiffness Analysis

Stiffness basically is the resistance of an elastic body to deformation by an applied force. It is an extensive material property. The stiffness, k , of a body is a measure of the resistance offered by an elastic body to deformation (bending, stretching or compression) [1].

$$k = \frac{F}{\delta} \quad \text{Eq. (9)}$$

Where,

- P is a steady force applied on the body.
- δ is the displacement produced by the force (for instance, the deflection of a beam, or the change in length of a stretched spring).

As both the applied force and displacement are vectors (respectively P and δ), in general their relationship is characterised by a stiffness matrix, k, where:

$$P = k\delta \quad \text{Eq. (10)}$$

The displacement can, in general, refer to a point distinct from that where the force is applied and a complicated structure will not deflect purely in the same direction as an applied force. The stiffness matrix enables such systems to be characterised in straightforward terms. The inverse of stiffness is compliance, typically measured in units of metres per Newton. In theology it may be defined as the ratio of strain to stress, and so take the units of reciprocal stress, e.g. 1/Pa [1].

2.4 Natural and Fundamental Frequency

Consider a beam, fixed at one end and having a mass attached to the other, this would be a single degree of freedom oscillator. Once set into motion it will oscillate at its natural frequency. For a single degree of freedom oscillator, a system in which the motion can be described by a single coordinate, the natural frequency depends on two system properties; mass and stiffness. The circular natural frequency, ω_n , can be found using the following equation, [1]

$$\omega_n^2 = \frac{k}{m} \quad \text{Eq. (11)}$$

Where,

- k = stiffness of the beam
- m = mass of weight
- ω_n = circular natural frequency (radians per second)

From the circular frequency, the natural frequency, f_n , can be found by simply dividing ω_n by 2π . Without first finding the circular natural frequency, the natural frequency can be found directly using:

$$f_n = \left(\frac{1}{2\pi}\right) \left(\frac{k}{m}\right)^{\frac{1}{2}} \quad \text{Eq. (12)}$$

Where,

- f_n = natural frequency in hertz (1/seconds)
- k = stiffness of the beam (Newton/Meters or N/m)
- m = mass of weight (kg)

2.5 Mode Shape

A mode shape describes the expected curvature (or displacement) of a surface vibrating at a particular mode. To determine the vibration of a system, the mode shape is multiplied by a function that varies with time, thus the mode shape always describes the curvature of vibration at all points in time, but the magnitude of the curvature will change. The mode shape is dependent on the shape of the surface as well as the boundary conditions of that surface. Typically, an object will vibrate at several modes at once, thus, assuming linear behaviour, the total displacement will be a superposition of the mode shapes of the individual modes. Each mode is multiplied by a different time function, such that all modes vibrate at a different frequency [1]. For example, a beam might have a mode shape of:

$$y_n(x) = \sin\left(\frac{\pi nx}{L}\right) \quad \text{Eq. (13)}$$

Where n is the mode number, x is the distance from a given end of the beam, and L is the overall length. The n subscript denotes that this is for a single n -th mode. The time function may look like:

$$y_n(t) = \sin\left(\frac{\pi nt}{T}\right) \quad \text{Eq. (14)}$$

Where t is time and T is the period of vibration. Thus the vibration for a given mode is given by:

$$y_n(x, t) = \sin\left(\frac{\pi nx}{L}\right) \sin\left(\frac{\pi nt}{T}\right) \quad \text{Eq. (15)}$$

Since the total vibration of the beam is given by the superposition of all modes, the total vibration for our example system is given by:

$$y_n(x, t) = \sum_{n=1}^{\infty} c_n \sin\left(\frac{\pi nx}{L}\right) \sin\left(\frac{\pi nt}{T}\right) \quad \text{Eq. (16)}$$

2.6 Dynamic Analysis

Analyses on motorcycle drum brake and brake shoe using the finite element method [2].

In this particular journal, finite element method was used to do dynamic analysis on the motorcycle drum brake and brake shoe. The natural frequencies and vibration modes of the two equipments have been determined using the decided method which is F.E.M. the vibration of these drum brake and brake shoe are related to the squeal noise generated by the motorcycle drum brake which is related to the perceived quality of the motorcycle and noise pollution. There have been a considerable number of works on drum brake squeal, and since, drum brake squeal analysis had being shown by the effect of modal intensity and the influence of various geometric parameters. The present work attempts to identify the design parameter of a motorcycle drum brake which influence its natural frequency in particular those parameters which can reduce the modal intensities and the diametral mode of the drum. A typical drum brake of a light motorcycle (110cc) of a Malaysian made is used in this analysis. A three-dimensional finite element model of the drum brake and brake shoe; consists of hexahedral elements with eight nodes. The definition of nodes and elements are created using ANSYS 6.0 finite element solver package. As a result, there are 42 mode shapes for the drum and 10 mode shapes for the shoe within the frequency range of 100 Hz and 12000 Hz [2].

Analysis of multi-step non-uniform bars using piecewise analytical solutions [3].

Using appropriate transformations, the differential equations of free longitudinal vibrations of bars with variably distributed mass and stiffness are reduced to Bessel's equations or ordinary differential equations with constant coefficients by selecting suitable expressions, such as power functions and exponential functions, for the distribution of stiffness and mass. Exact analytical solutions to determine the longitudinal natural frequencies and mode shapes for a one step non-uniform bar are derived and used to obtain the frequency equation of a multi-step non-uniform bar with several boundary conditions. This approach which combines the transfer matrix method and closed-form solutions of one step non-uniform bars lead to a single frequency equation for any number of steps. Numerical

example show that the computed values of the longitudinal fundamental natural frequencies and mode shapes of a tall building by the proposed method are close to the field measured data.

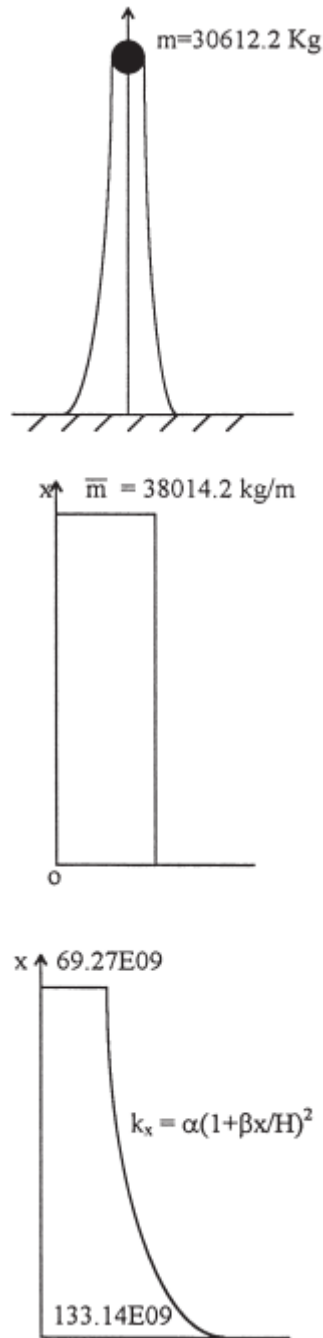


Figure 2.3: (a) The tall building is simplified as a one-step bar; (b) mass distribution; (c) stiffness distribution [3]

It is also demonstrated through the numerical example that the selected expressions are suitable for describing the distributions of stiffness and mass of typical tall buildings. The exact analytical solutions describing the longitudinal vibration of one-step bars with variably distributed stiffness and mass are derived.

The obtained analytical solutions are used to establish the frequency equation of a multi-step non-uniform bar with several boundary conditions. This approach for determining structural dynamic characteristics of a multi-step non-uniform bar that combines the transfer matrix method and closed-form solutions of one-step non-uniform bars lead to a single frequency equation for any number of steps. Using the proposed formulas for determining free longitudinal vibration of a one-step cantilever beam with variably distributed stiffness and mass obtains that the fundamental natural frequency gained. The evaluated distribution of stiffness is shown in Figure 2.3 [3].

It is obvious that the difference between the results calculated by use of the step varying distributions of stiffness and mass and those obtained based on the model of a one-step cantilever bar with continuously varying stiffness and mass is so small that it can be neglected. This suggests that it is reasonable to simplify a multi-step bar with step varying distributions of stiffness and mass as a one-step bar with continuously distributed stiffness and mass for free vibration analysis when the number of step is large.

2.7 Micro Unmanned Aerial Vehicle (UAV) Design

The design had been obtain from one of the final year final semester July 2009 student who did FYP of designing the Micro UAV structure using AutoCAD software..

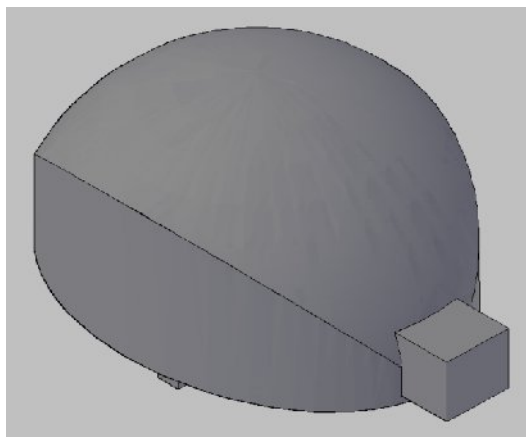


Figure 2.4: Micro UAV 3D Solid Structure [4]

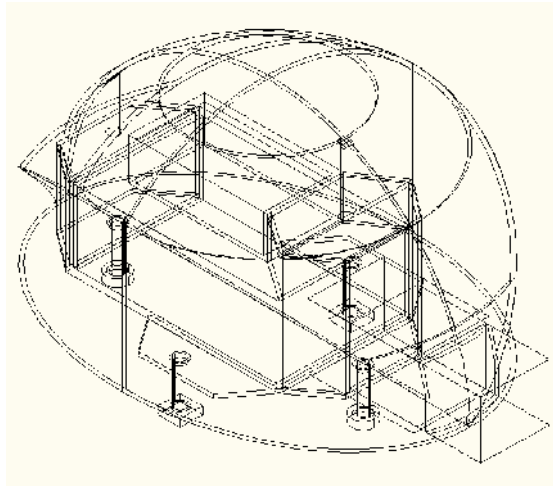


Figure 2.5: Micro UAV 3D Wired Structure [4]

Table 2.1: Design specification of Micro UAV [4]

No	Specification	Description
1	Size	<p>5" X 3" (12.7cm X 7.6cm)</p> <p>Small size is required for micro UAV. The required size is not more than 6 inches (15cm).</p>
2	Weight	<p>≈ 200 grams</p> <p>This is the limit estimated weight of this micro UAV. It depends on structure and the engine that will power up this micro UAV. Less weight can use small engine capacity to lift.</p>
3	Provision	<p>Power Pack*</p> <p>Thunder Power 2100mAh 2S3PR 7.4V Lithium Polymer Receiver Battery Pack</p> <p>Size = 55mm X 33mm X 19mm</p> <p>Weight ≈ 70gram</p>

		<p>Controller*</p> <p><i>Futaba 6EX-PCM 6 Channel Receiver</i></p> <p>Size = 34mm X 18mm X 10mm</p> <p>Weight \cong 20gram</p> <p>Camera vision*</p> <p>RC-12-mini-spy camera</p> <p>Size = 35mmX18mmX15mm</p> <p>Weight \cong 20gram</p> <p>*(All the provision base on air craft RC)</p>
4	Material	<p>Light weight</p> <p>To make sure the weight cannot more than 0.2 kg, the light weight material is required as the part of design body.</p>
5	Design	<p>Small design with vertical take-off and landing gear attached.</p>

CHAPTER 3 METHODOLOGY

3.1 Project Flowchart

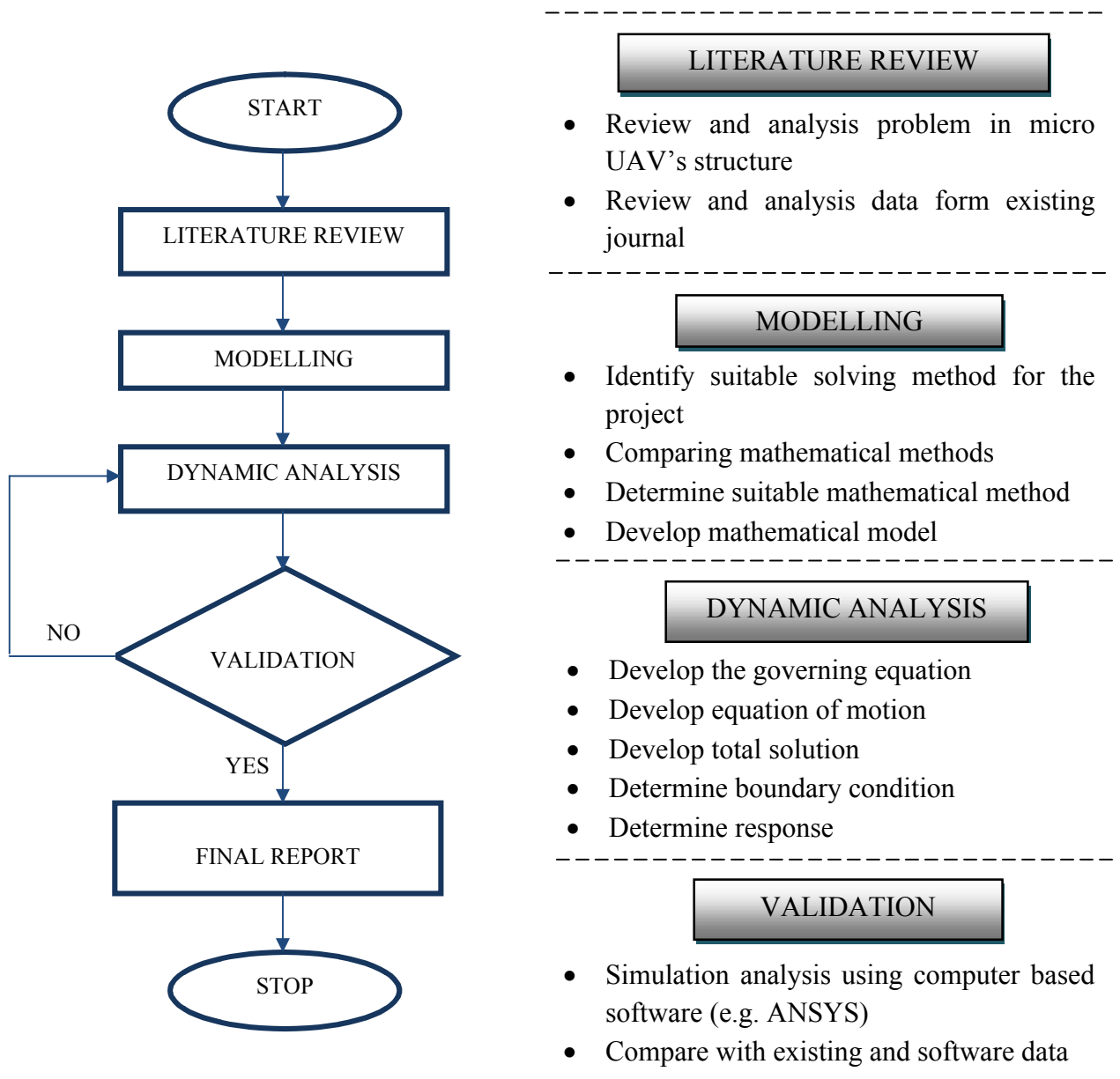


Figure 3.1: Project Methodology Flowchart

3.2 Project Methodology Sequences

Since this is a research and an analysis project, therefore the project should be done step-by-step so that all tasks done are clearly understood and a good result can be obtained. The methodology is as follow. First of all, a thorough research will be done regarding the dynamic analysis. A comprehensive study and reading will be implemented on the fundamental of a dynamic continuous system. The study provide the information of behavior and the respond (displacement) of the continuous system and also the method of finding the natural frequency and mode shape of a continuous system. The literature review will be done from the previous papers and journal which are related to the dynamics analysis of a structure. Most of the Micro UAV structure design will be obtain from consultation with supervisor and Micro UAV team.

After the reviews of the literature being completed, the project methodology will be developed. As time to time, the literature reviews will be updated in order to make the analysis research more reliable. In the methodology, the best suitable method will be implemented to find the natural frequency and mode shape. After the mathematical modeling has been developed, the suitable software will be used to test and validate all data that had been gathered. If the analysis was perfect, the result will be compared to existing journal with similar method in dynamic analysis for validation process. If not, the mathematics will be calculated again and being simulated then.

After the result had been finalized true and can be used, different input values will be used. The first one will be the effect of the material that being used. The result between material such as plastic and aluminum will be compared in order to analyze the better result. Then, the effect of geometry of the Micro UAV structure will be utilized. This is to get the best solution for the Micro UAV structure.

Finally, the data and results that created will be rearranging and altered in order to make it more presentable for the use of researchers, lecturers, students of university and public.

3.3 Tools / Equipments Required

The tools and equipment which are required in this Final Year Project are a Windows based PC together with the programs such as Microsoft Office which is used to analyse the data obtained from the site, equipment needed basically would be data from on site results as well as from the internet and other references.

The software's that may be required to achieve the objectives of this project are as follow:

- Autodesk AutoCAD & Inventor for drawing, analysis and presentation.
- ANSYS for analysis and simulation.
- MATLAB for analysis and simulation.

3.4 Materials Properties

ABS is an amorphous thermoplastic blend. The recipe is 15-35% acrylonitrile, 5-30% butadiene and 40-60% styrene. Depending on the blend different properties can be achieved.

Acrylonitrile contributes with thermal and chemical resistance, and the rubberlike butadiene gives ductility and impact strength. Styrene gives the glossy surface and makes the material easily machinable and less expensive.

Generally, ABS has good impact strength also at low temperatures. It has satisfactory stiffness and dimensional stability, glossy surface and is easy to machine. It is often used for refrigerator door liners, interior automotive trim, coextruded sheets capped with a weather able polymer, and housings for business machines, small appliances, telephones, and other consumer electronics.

Table 3.1: ABS Properties [4]

GENERAL PROPERTIES				
Density	1010	-	1210	kg/m ³
Price	2.511	-	2.952	USD/kg
MECHANICAL PROPERTIES				
Young's modulus	1.1	-	2.9	GPa
Shear modulus	0.3189	-	1.032	Gpa
Bulk modulus	3.8	-	4	Gpa
Poisson's ratio	0.3908	-	0.422	
Yield strength (elastic limit)	18.5	-	51	Mpa
Tensile strength	27.6	-	55.2	Mpa
Compressive strength	31	-	86.2	Mpa
Elongation	1.5	-	100	%
Hardness – Vickers	5.6	-	15.3	HV
Fatigue strength at 10 ⁷ cycles	11.04	-	22.08	Mpa
Fracture toughness	1.186	-	4.289	MP a.m ^{1/2}
Mechanical loss coefficient	0.01379	-	0.04464	

3.5 Micro Unmanned Aerial Vehicle (UAV) Structure Properties

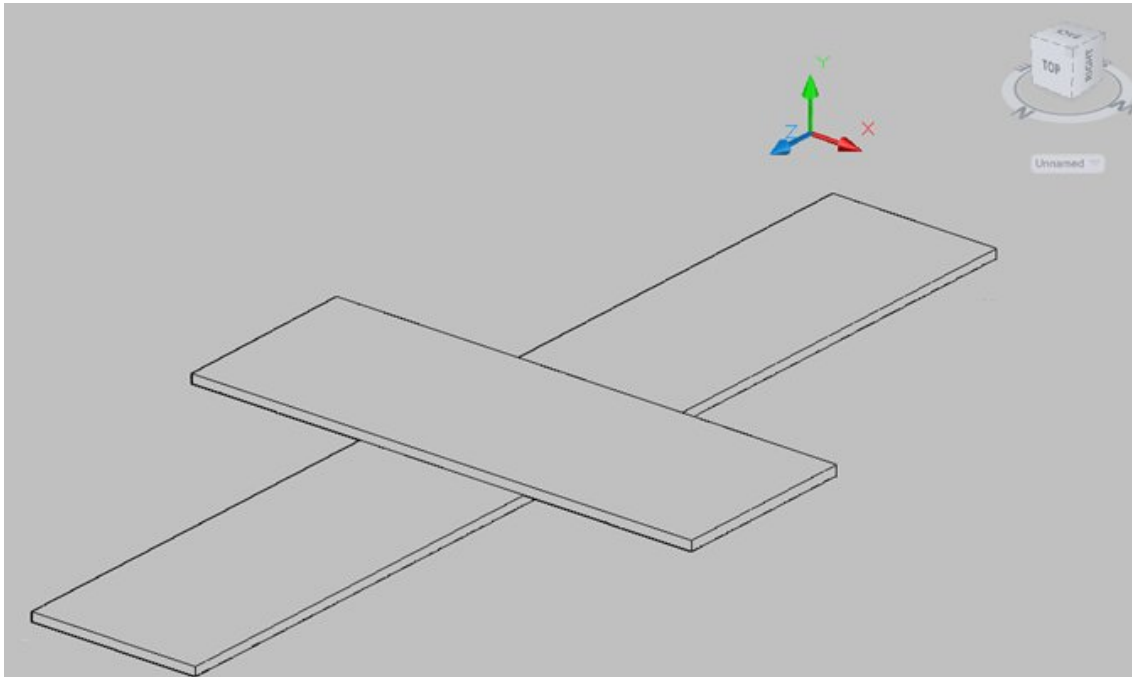


Figure 3.2: Micro UAV Structure

Detail of Structure:

- 2 Beams (The upper beam rest on top in the middle of the lower beam).
- Each beam carried 2 fans, each fan at the end of the beam.
- All equipments of Micro UAV positioned on top of the upper beam.

3.5.1 Upper Beam

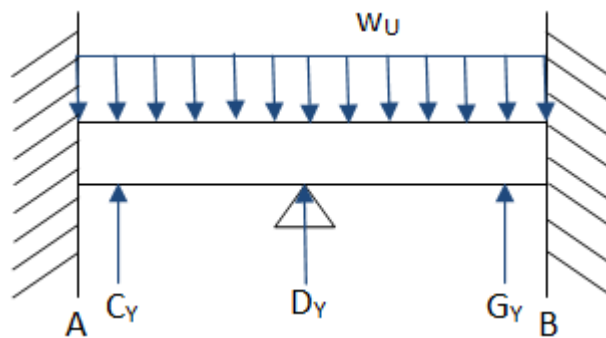


Figure 3.3: Schematic Diagram of the Upper Beam

Detail of Upper Beam:

E , Modulus of elasticity: 2.9 Gpa

ρ , Density: 1210 kg/m^3

I , Moment of Inertia: $1.33 \times 10^{-9} \text{ m}^4$

m , Mass of beam: 0.002662 kg

L , Total length: 0.055 m

Distance C_Y and $A =$ Distance G_Y and $B = 0.005\text{ m}$

Fixed end at both end and simply supported in the middle.

Distribution mass loading:

$$W_U = \frac{m \cdot g}{L}, \quad \text{take } g = 10\text{ m/s}^2$$

$$W_U = 0.484\text{ N/m}$$

To determine the value of C_Y , D_Y and G_Y , method superposition is used to solve the problem. First, we chose which forces are redundant.

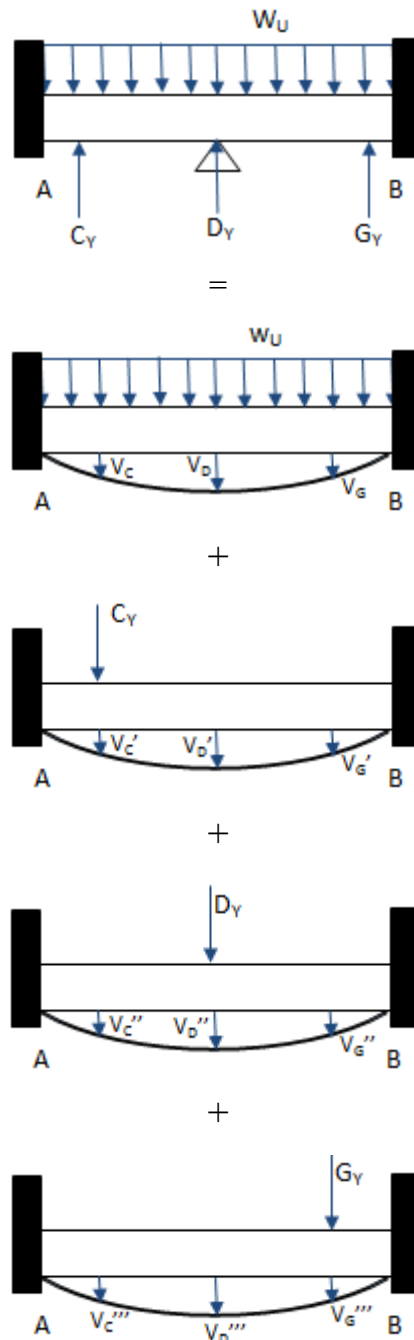


Figure 3.4: Superposition Method for Upper Beam [5]

The forces at C , D and G are redundant. The primary beam and each redundant force deform this beam in Figure 3.4, respectively. By superposition, the compatibility equations for the displacements at C , D and G are

$$0 = v_C + v_C' + v_C'' + v_C''' \quad \text{Eq. (17)}$$

$$0 = v_D + v_D' + v_D'' + v_D''' \quad \text{Eq. (18)}$$

$$0 = v_G + v_G' + v_G'' + v_G''' \quad \text{Eq. (19)}$$

Using the information from Appendix A, hence, the displacement components v_C' , v_D' , and v_G' will be expressed in terms of the unknown C_Y ; the components v_C'' , v_D'' , and v_G'' will be expressed in terms of the unknown D_Y , and for the components v_C''' , v_D''' , and v_G''' , will be determined in terms of the unknown G_Y .

When these displacements have been determined and substituted into Equation (17), (18) and (19), the equations are as below,

$$9.80E^{-8}C_Y - 0.00081D_Y - 3.9E^{-6}G_Y + 4.27E^{-9} = 0 \quad \text{Eq. (20)}$$

$$2.42E^{-7}C_Y + 8.96E^{-7}D_Y - 2.5E^{-7}G_Y + 1.49E^{-8} = 0 \quad \text{Eq. (21)}$$

$$5.83E^{-8}C_Y - 7.8E^{-5}D_Y + 9.80E^{-8}G_Y + 4.27E^{-9} = 0 \quad \text{Eq. (22)}$$

By substituting Equation (20), (21), and (22) into matrix form, the value of C_Y , D_Y and G_Y will be determined.

$$+\downarrow C_Y = 0.06337 \text{ N} \quad \text{Eq. (23)}$$

$$+\uparrow D_Y = 5.341E^{-6} \text{ N} \quad \text{Eq. (24)}$$

$$+\downarrow G_Y = 0.0016178 \text{ N} \quad \text{Eq. (25)}$$

Substituting all the values into free body diagram, the new FBD is as below,

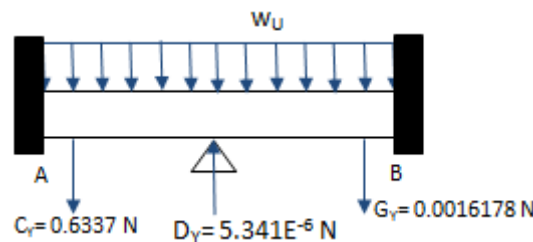


Figure 3.5: Free Body Diagram of the Upper Beam

3.5.2 Lower Beam

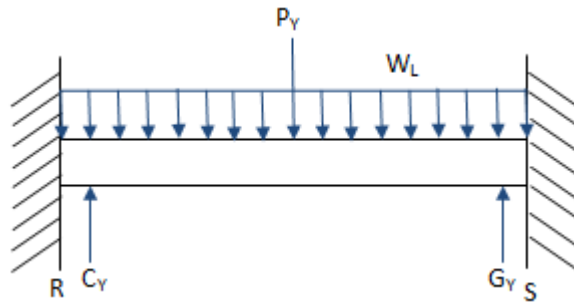


Figure 3.6: Schematic Diagram of the Lower Beam

Detail of Lower Beam:

E , Modulus of elasticity: 2.9 Gpa

ρ , Density: 1210 kg/m^3

I , Moment of Inertia: $0.972 \times 10^{-9} \text{ m}^4$

m , Mass of beam: 0.002662 kg

L , Total length: 0.112 m

Distance C_Y and $A =$ Distance G_Y and $B = 0.005 \text{ m}$

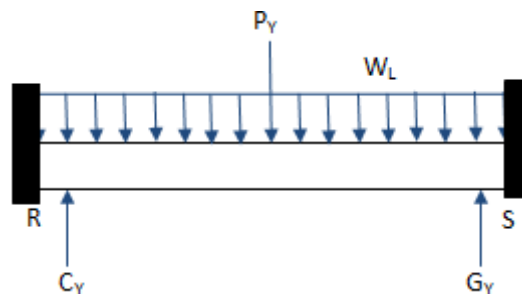
Fixed end at both end and simply supported in the middle.

Distribution mass loading:

$$W_U = \frac{m \cdot g}{L}, \quad \text{take } g = 10 \text{ m/s}^2$$

$$W_U = 0.4356 \text{ N/m}$$

To determine the value of C_Y and G_Y , method superposition is used to solve the problem. First, we chose which forces are redundant.



=

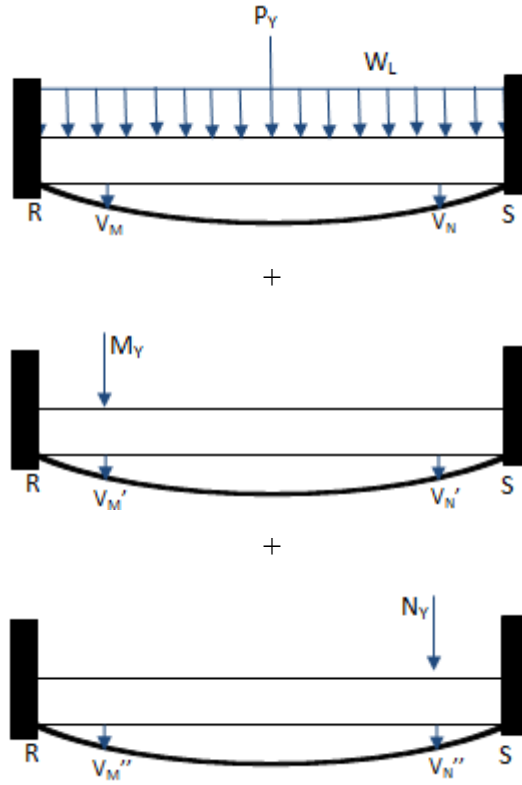


Figure 3.7: Superposition Method for the Upper Beam [5]

The forces at $C_Y = M$ and $G_Y = N$ are redundant. The primary beam and each redundant force deform this beam in Figure (3.7), respectively. By superposition, the compatibility equations for the displacements at M and N are

$$0 = v_M + v_M' + v_M'' \quad \text{Eq. (26)}$$

$$0 = v_N + v_N' + v_N'' \quad \text{Eq. (27)}$$

Using the information from Appendix A, hence, the displacement components v_M' and v_N' will be expressed in terms of the unknown M_Y , and the components v_M'' and v_N'' will be expressed in terms of the unknown N_Y . When these displacements have been determined and substituted into Equation (26) and (27), the equations are as below,

$$1.22E^{-8}M_Y - 6.3E^{-5}N_Y + 4.51E^{-8} = 0 \quad \text{Eq. (28)}$$

$$2.8E^{-6}M_Y + 3.02E^{-7}N_Y - 9.2E^{-7} = 0 \quad \text{Eq. (29)}$$

By substituting Equation (28) and (29) into matrix form, the value of M_Y and N_Y will be determined.

$$+\uparrow M_Y = 0.32894 N \quad \text{Eq. (30)}$$

$$+\uparrow N_Y = 0.00078 \text{ N} \quad \text{Eq. (31)}$$

Substituting all the values into free body diagram, the new FBD is as below,

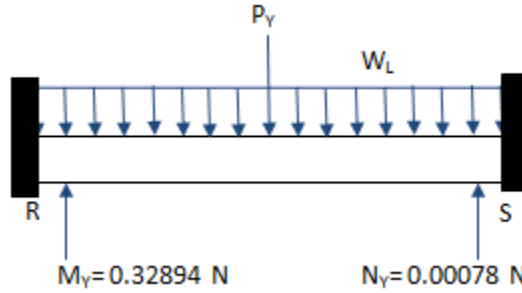


Figure 3.8: Free Body Diagram of the Lower Beam

3.6 Dynamic Analysis (Force Transfer Through Out the Beams)

3.6.1 Deriving the Equation of Motion

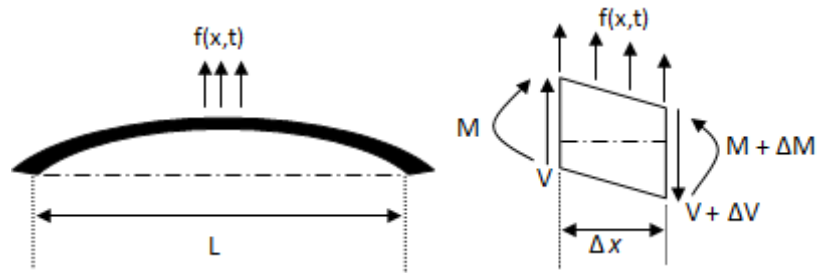


Figure 3.9: A Bending Beam [6]

The Figure 3.9 shows a beam subjected to an external force $f(x,t)$ per unit length. The beam vibrates laterally and its vertical displacement in the y direction is denoted as $w(x,t)$. $M(x,t)$ is the bending moment and $V(x,t)$ is the shear force. The beam has a Young's modulus E , a mass density ρ , a cross-sectional area A and an area moment of inertia I about the axis perpendicular to the plane x - y [6].

Applying Newton's second law in the y direction gives,

$$\sum F_y = m\hat{w}_y \quad \text{Eq. (32)}$$

$$\sum M_c \approx 0 \quad \text{Eq. (33)}$$

Where, m is the mass, equal to $\rho A \Delta x dx$ and \hat{w} is the acceleration in the y direction,

$$\hat{w} = \frac{\delta^2 w}{\delta t^2}. \quad \text{Eq. (34)}$$

Summing the forces in Figure (3.9), Equation (32) becomes

$$-(V + \Delta V) + f\Delta x + V = \rho A \Delta x \frac{\delta^2 w}{\delta t^2} \quad \text{Eq. (35)}$$

For the moment equation, Equation (33), applying to about the axis perpendicular to the plane x-y gives,

$$(M + \Delta M) - (V + \Delta V)\Delta x + f\Delta x \frac{\Delta x}{2} - M = 0 \quad \text{Eq. (36)}$$

For an infinitesimal length Δx , the terms of ΔV and ΔM are expressed as

$$\Delta V = \frac{\partial V}{\partial x} \Delta x, \quad \Delta M = \frac{\partial M}{\partial x} \Delta x \quad \text{Eq. (37)}$$

Ignoring the terms involving the second power of Δx , by substituting Equation (37) into Equation (35) and (36) gives,

$$-\frac{\partial V}{\partial x} + F = \rho A \frac{\delta^2 w}{\delta t^2} \quad \text{Eq. (38)}$$

$$\frac{\partial M}{\partial x} = V \quad \text{Eq. (39)}$$

Substituting Equation (39) into Equation (38) yields

$$-\frac{\partial^2 M}{\partial x^2} + F = \rho A \frac{\delta^2 w}{\delta t^2} \quad \text{Eq. (40)}$$

From Euler-Bernoulli theory, the bending moment can be considered as

$$M = EI \frac{\delta^2 w}{\delta x^2} \quad \text{Eq. (41)}$$

Substituting Equation (41) into Equation (40), obtaining the following equation of motion,

$$\frac{\partial^2}{\partial x^2} \left[EI \frac{\delta^2 w}{\delta x^2} \right] + \rho A \frac{\delta^2 w}{\delta t^2} = F \quad \text{Eq. (42)}$$

In case of a uniform beam, Equation (42) becomes,

$$EI \frac{\delta^4 w}{\delta x^4} + \rho A \frac{\delta^2 w}{\delta t^2} = F \quad \text{Eq. (43)}$$

Or

$$c^2 \frac{\delta^4 w}{\delta x^4} + \frac{\delta^2 w}{\delta t^2} = F_o \sin \omega_f t \quad \text{Eq. (44)}$$

Where, $c = \left(\frac{EI}{\rho A}\right)^{\frac{1}{2}}$ and $F = F_0 \sin \omega_f t$.

The Equation (44) is expressed as the equation of motion of a uniform subjected to the harmonic force, where ω_f is the frequency, in radian per second.

3.6.2 Total Response Equation

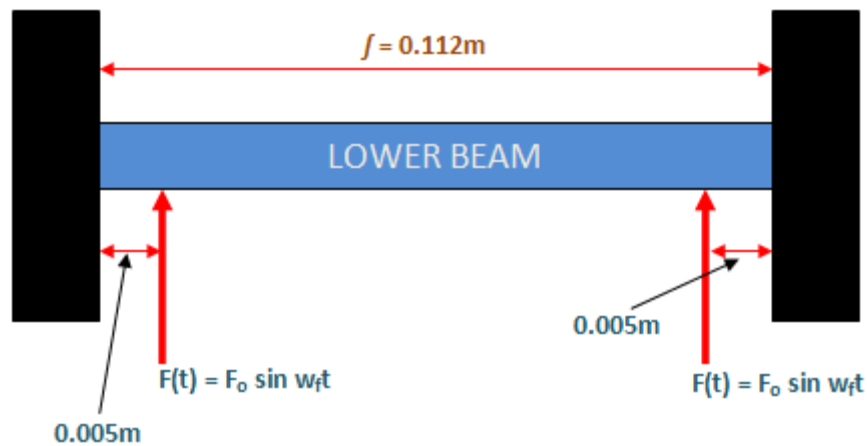


Figure 3.10: Lower Beam System with Harmonic Force

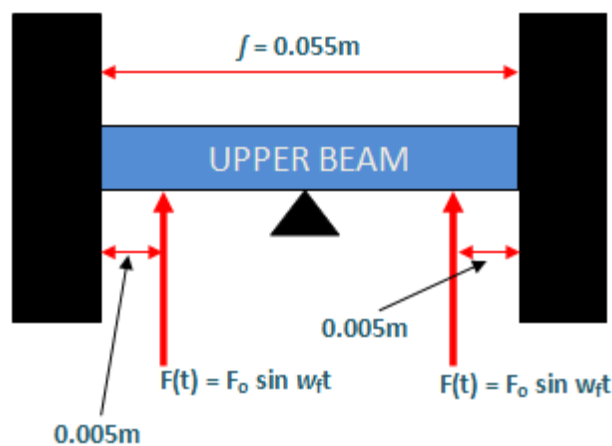


Figure 3.11: Upper Beam System with Harmonic Force

As both beams are being considered in position as stated in the figures above, loaded with external harmonic force $F(t)$, which is supplied by the fans:

$$F(t) = F \sin \omega_f t \quad \text{Eq. (45)}$$

There are some assumptions which applied in order to solve the problem. The assumptions are listed below:

1. The ends of both beams are considered fixed end (attached to the casing of the Micro UAV).
2. Total weight of the upper beam including all equipments of Micro UAV is concentrated on top of the middle of the lower beam.
3. There is a pinned support at the middle of the upper beam, supported by the lower beam.
4. There is no outside force exerted onto the structure except the harmonic force from the fan itself.
5. ω_f is the frequency of the harmonic force from the fan blade which is obtain for frequency range of (0Hz – 30 Hz).
6. The time duration for each dynamic analysis is been fixed up to 900 sec or 15 minutes.
7. The amplitude of the harmonic force is a constant value of 0.4N, which is the mass of the fan times g, $0.04 \text{ kg} \times 10 \text{ m/s}^2 = 0.4\text{N}$.
8. Fan is situated 0.005m from each end of the beams.
9. Analyses are being done separately beam by beam.

Considering the harmonic force supplied, the steady-state motion will be determined. We assume the total response, $w(x,t)$ of each beam (upper and lower beam), using the method of separation of variables to be the form of:

$$w(x, t) = W(x) T(t) \quad \text{Eq. (46)}$$

where, the function $W(x)$ depends only on x and the function $T(t)$ depends only on t .

Substituting Equation (46) into Equation (44) and rearranging leads to

$$\frac{c^2}{W(x)} \frac{d^4 W(x)}{dx^4} = -\frac{1}{T(t)} \frac{d^2 T(t)}{dt^2} = \alpha = \omega^2 \quad \text{Eq. (47)}$$

where, the constant α and ω^2 are positive numbers. α is chosen to be equal to ω^2 because it is the only value that gives a physically acceptable solution for the two

partial differential equations in Equation (46). Since ω^2 is a positive, and cannot be equal to zero, then Equation (46) can be separated into two equations, yields:

$$\frac{d^4 W(x)}{dx^4} - \beta^4 W(x) = 0, \text{ and} \quad \text{Eq. (48)}$$

$$\frac{d^2 T(t)}{dt^2} + \omega^2 T(t) = 0 \quad \text{Eq. (49)}$$

Where, the variable β^4 is given by:

$$\beta^4 = \frac{\omega^2}{c^2} = \frac{\rho A \omega^2}{EI} \quad \text{Eq. (50)}$$

Not forgetting, Equation (49) can be expressed as

$$T(t) = A \cos \omega t + B \sin \omega t \quad \text{Eq. (51)}$$

Where A and B are constants that can be found from the initial conditions, or since the applied force is a sinusoidal, the Equation (51) can be best describe as

$$T(t) = \sin \omega_f t \quad \text{Eq. (52)}$$

Substituting Equation (52) into Equation (49), yields:

$$\omega^2 = \omega_f^2 \quad \text{Eq. (53)}$$

For the solution of Equation (48), assume

$$W(x) = C e^{sx} \quad \text{Eq. (54)}$$

Where C and S are constants, so deriving the auxiliary equation as

$$s^4 - \beta^4 = 0 \quad \text{Eq. (55)}$$

The roots that will be obtained from Equation (55) are

$$s_{1,2} = \pm \beta, \quad s_{3,4} = \pm i\beta \quad \text{Eq. (56)}$$

From the assumption that had being done, hence the solution for Equation (54) becomes

$$W(x) = C_1 e^{-i\beta x} + C_2 e^{i\beta x} + C_3 e^{-\beta x} + C_4 e^{\beta x} \quad \text{Eq. (57)}$$

Where, C_1 , C_2 , C_3 , and C_4 are constants. Equation (57) can also be expressed as

$$W(x) = C_1 \sinh \beta x + C_2 \cosh \beta x + C_3 \sin \beta x + C_4 \cos \beta x \quad \text{Eq. (58)}$$

Therefore, the values of C_1 , C_2 , C_3 , and C_4 above can be found from the boundary conditions.

$$\beta^4 = \frac{\rho A \omega_f^2}{EI} \quad \text{Eq. (59)}$$

From the Equation (59), the value of β can be found.

3.7 Boundary Condition

Before we can proceed with estimating the boundary condition applied to the beam, we need to clarify the assumption that we want to assume to each of the beam, so that we can understand the condition that originally applied to the structure. For both beams, whereby there is a force acting onto the beam cause by the force supplied from the fan, that point is considered free end boundary condition and having external load from the wind.

3.7.1 Lower Beam

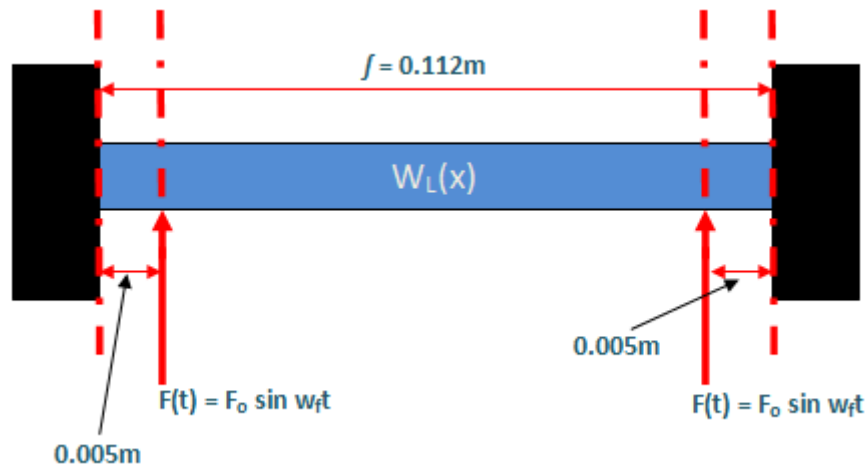


Figure 3.12: Lower Beam's Boundary Condition with Harmonic Force

In the scenario above, $W_L(x)$ applied along the beam, so the mode shape can be define as

$$W_L(x) = C_1 \sinh \beta x + C_2 \cosh \beta x + C_3 \sin \beta x + C_4 \cos \beta x \quad \text{Eq. (60)}$$

So, from Equation (59), the total response for the lower beam is

$$w_L(x, t) = W_L(x) T(t) \quad \text{Eq. (61)}$$

All constants, $C_1, C_2, C_3,$ and C_4 can be found utilizing the boundary condition applied and the value of β .

The boundary conditions are stated as below:

From left, at $x = 0 \text{ m}$ (Fixed End);

- Deflection, $W_L(x) = 0$
- Slope, $\frac{dW_L(x)}{dx} = 0$

At $x = 0.005 \text{ m}$;

- Bending moment, $EI \frac{d^2 W_L(x)}{dx^2} = 0$
- Shear force, $-EI \frac{d^3 W_L(x)}{dx^3} = F_1$

At $x = 0.107 \text{ m}$;

- Bending moment, $EI \frac{d^2 W_L(x)}{dx^2} = 0$
- Shear force, $-EI \frac{d^3 W_L(x)}{dx^3} = F_2$

At $x = 0.112 \text{ m}$ (Fixed End);

- Deflection, $W_L(x) = 0$
- Slope, $\frac{dW_L(x)}{dx} = 0$

From Equation (59), it can be derived into;

$$W_L(x) = C_1 \sinh \beta x + C_2 \cosh \beta x + C_3 \sin \beta x + C_4 \cos \beta x \quad \text{Eq. (62)}$$

$$\frac{dW_L(x)}{dx} = C_1 \beta \cosh \beta x + C_2 \beta \sinh \beta x + C_3 \beta \cos \beta x - C_4 \beta \sin \beta x \quad \text{Eq. (63)}$$

$$\frac{d^2 W_L(x)}{dx^2} = C_1 \beta^2 \sinh \beta x + C_2 \beta^2 \cosh \beta x - C_3 \beta^2 \sin \beta x - C_4 \beta^2 \cos \beta x \quad \text{Eq. (64)}$$

$$\frac{d^3 W_L(x)}{dx^3} = C_1 \beta^3 \cosh \beta x + C_2 \beta^3 \sinh \beta x - C_3 \beta^3 \cos \beta x + C_4 \beta^3 \sin \beta x \quad \text{Eq. (65)}$$

Then, from the derivative equations that had been yield and Equation (62), (63), (64) and (65), using respective boundary conditions, the most 4 simple equations are:

Deflection, $W_L(x) = 0; x = 0 \text{ m}$

$$C_1 \sinh(\beta x 0) + C_2 \cosh(\beta x 0) + C_3 \sin(\beta x 0) + C_4 \cos(\beta x 0) = 0 \quad \text{Eq. (66)}$$

Shear Force, $-EI \frac{d^3 W_L(x)}{dx^3} = F_1; x = 0.005 \text{ m}$

$$C_1 \beta^3 \cosh(\beta x 0.005) + C_2 \beta^3 \sinh(\beta x 0.005) - C_3 \beta^3 \cos(\beta x 0.005) + C_4 \beta^3 \sin(\beta x 0.005) = \frac{-F_1}{EI}$$

$$\text{Eq. (67)}$$

Shear Force, $-EI \frac{d^3 W_L(x)}{dx^3} = F_2; x = 0.107 \text{ m}$

$$C_1 \beta^3 \cosh(\beta x 0.107) + C_2 \beta^3 \sinh(\beta x 0.107) - C_3 \beta^3 \cos(\beta x 0.107) + C_4 \beta^3 \sin(\beta x 0.107) = \frac{-F_2}{EI}$$

$$\text{Eq. (68)}$$

Deflection, $W_L(x) = 0; x = 0.112 \text{ m}$

$$C_1 \sinh(\beta x 0.112) + C_2 \cosh(\beta x 0.112) + C_3 \sin(\beta x 0.112) + C_4 \cos(\beta x 0.112) = 0 \quad \text{Eq. (69)}$$

$$\text{With } \beta^4 = \frac{\rho A \omega_f^2}{EI} \quad \text{Eq. (70)}$$

Substituting Equation (66), (67), (68), and (69) into matrix form;

$$\begin{bmatrix} \sinh(\beta x 0) & \cosh(\beta x 0) & \sin(\beta x 0) & \cos(\beta x 0) \\ \beta^3 \cosh(\beta x 0.005) & \beta^3 \sinh(\beta x 0.005) & -\beta^3 \cos(\beta x 0.005) & \beta^3 \sin(\beta x 0.005) \\ \beta^3 \cosh(\beta x 0.107) & \beta^3 \sinh(\beta x 0.107) & -\beta^3 \cos(\beta x 0.107) & \beta^3 \sin(\beta x 0.107) \\ \sinh(\beta x 0.112) & \cosh(\beta x 0.112) & \sin(\beta x 0.112) & \cos(\beta x 0.112) \end{bmatrix} \times \begin{bmatrix} C_1 \\ C_2 \\ C_3 \\ C_4 \end{bmatrix} = \begin{bmatrix} 0 \\ \frac{-F_1}{EI} \\ \frac{-F_2}{EI} \\ 0 \end{bmatrix} \quad \text{Eq. (71)}$$

The value of ω_f is between 0 Hz to 30 Hz, and choosing value of 5 Hz, 10 Hz, 15 Hz, 20 Hz, 25 Hz and 30 Hz, the matrix is being solved using inverse matrix method. All constant value can be determined and stated in the tables in section 4.1.

3.7.2 Upper Beam

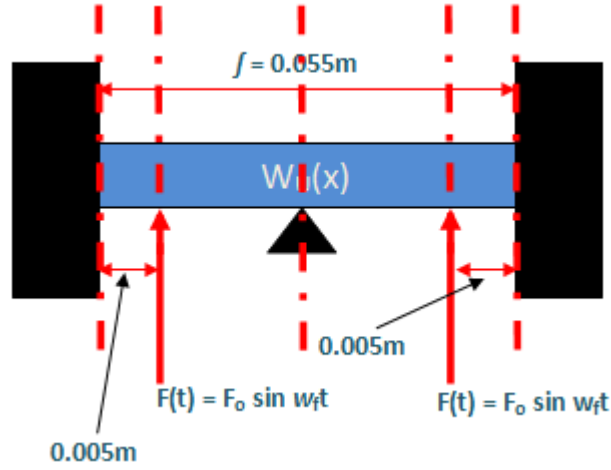


Figure 3.13: Upper Beam's Boundary Condition with Harmonic Force

In the scenario above, $W_U(x)$ applied along the beam, so the mode shape can be define as

$$W_U(x) = C_1 \sinh \beta x + C_2 \cosh \beta x + C_3 \sin \beta x + C_4 \cos \beta x \quad \text{Eq. (72)}$$

So, from Equation (72), the total response for the upper beam is

$$w_U(x, t) = W_U(x) T(t) \quad \text{Eq. (73)}$$

All constants, $C_1, C_2, C_3,$ and C_4 can be found utilizing the boundary condition applied and the value of β .

The boundary conditions are stated as below:

From left, at $x = 0 \text{ m}$ (Fixed End);

- Deflection, $W_U(x) = 0$
- Slope, $\frac{dW_U(x)}{dx} = 0$

At $x = 0.005 \text{ m}$;

- Bending moment, $EI \frac{d^2 W_U(x)}{dx^2} = 0$
- Shear force, $-EI \frac{d^3 W_U(x)}{dx^3} = F_3$

At $x = 0.0275 \text{ m}$;

- Deflection, $W_U(x) = 0$
- Bending moment, $EI \frac{d^2 W_U(x)}{dx^2} = 0$

At $x = 0.05 \text{ m}$;

- Bending moment, $EI \frac{d^2 W_U(x)}{dx^2} = 0$

- Shear force, $-EI \frac{d^3 W_U(x)}{dx^3} = F_4$

At $x = 0.055 \text{ m}$ (Fixed End);

- Deflection, $W_U(x) = 0$
- Slope, $\frac{dW_U(x)}{dx} = 0$

From Equation (70), it can be derived into;

$$W_U(x) = C_1 \sinh \beta x + C_2 \cosh \beta x + C_3 \sin \beta x + C_4 \cos \beta x \quad \text{Eq. (74)}$$

$$\frac{dW_U(x)}{dx} = C_1 \beta \cosh \beta x + C_2 \beta \sinh \beta x + C_3 \beta \cos \beta x - C_4 \beta \sin \beta x \quad \text{Eq. (75)}$$

$$\frac{d^2 W_U(x)}{dx^2} = C_1 \beta^2 \sinh \beta x + C_2 \beta^2 \cosh \beta x - C_3 \beta^2 \sin \beta x - C_4 \beta^2 \cos \beta x \quad \text{Eq. (76)}$$

$$\frac{d^3 W_U(x)}{dx^3} = C_1 \beta^3 \cosh \beta x + C_2 \beta^3 \sinh \beta x - C_3 \beta^3 \cos \beta x + C_4 \beta^3 \sin \beta x \quad \text{Eq. (77)}$$

Then, from the derivative equations that had been yield and Equation (74), (75), (76) and (77), using respective boundary conditions, the most 4 simple equations are:

Deflection, $W_U(x) = 0; x = 0 \text{ m}$

$$C_1 \sinh(\beta x 0) + C_2 \cosh(\beta x 0) + C_3 \sin(\beta x 0) + C_4 \cos(\beta x 0) = 0 \quad \text{Eq. (78)}$$

Shear Force, $-EI \frac{d^3 W_U(x)}{dx^3} = F_3; x = 0.005 \text{ m}$

$$C_1 \beta^3 \cosh(\beta x 0.005) + C_2 \beta^3 \sinh(\beta x 0.005) - C_3 \beta^3 \cos(\beta x 0.005) + C_4 \beta^3 \sin(\beta x 0.005) = \frac{-F_3}{EI} \quad \text{Eq. (79)}$$

Bending moment, $EI \frac{d^2 W_U(x)}{dx^2} = 0; x = 0.0275 \text{ m}$

$$C_1 \beta^2 \sinh(\beta x 0.0275) + C_2 \beta^2 \cosh(\beta x 0.0275) - C_3 \beta^2 \sin(\beta x 0.0275) - C_4 \beta^2 \cos(\beta x 0.0275) = 0 \quad \text{Eq. (80)}$$

Shear Force, $-EI \frac{d^3 W_U(x)}{dx^3} = F_4; x = 0.05 \text{ m}$

$$C_1 \beta^3 \cosh(\beta x 0.05) + C_2 \beta^3 \sinh(\beta x 0.05) - C_3 \beta^3 \cos(\beta x 0.05) + C_4 \beta^3 \sin(\beta x 0.05) = \frac{-F_4}{EI} \quad \text{Eq. (81)}$$

$$\text{With } \beta^4 = \frac{\rho A \omega_f^2}{EI} \quad \text{Eq. (82)}$$

Substituting Equation (78), (79), (80), and (81) into matrix form;

$$\begin{bmatrix}
 \sinh(\beta x 0) & \cosh(\beta x 0) & \sin(\beta x 0) & \cos(\beta x 0) \\
 \beta^3 \cosh(\beta x 0.005) & \beta^3 \sinh(\beta x 0.005) & -\beta^3 \cos(\beta x 0.005) & \beta^3 \sin(\beta x 0.005) \\
 \sinh(\beta x 0.0275) & \cosh(\beta x 0.0275) & -\sin(\beta x 0.0275) & -\cos(\beta x 0.0275) \\
 \beta^3 \cosh(\beta x 0.05) & \beta^3 \sinh(\beta x 0.05) & -\beta^3 \cos(\beta x 0.05) & \beta^3 \sin(\beta x 0.05)
 \end{bmatrix}$$

$$\times \begin{bmatrix} C_1 \\ C_2 \\ C_3 \\ C_4 \end{bmatrix} = \begin{bmatrix} 0 \\ -F_2 \\ EI \\ 0 \\ -F_4 \\ EI \end{bmatrix} \quad \text{Eq. (83)}$$

The value of ω_f is between 0 Hz to 30 Hz, and choosing value of 5 Hz, 10 Hz, 15 Hz, 20 Hz, 25 Hz and 30 Hz, the matrix is being solved using inverse matrix method. All constant value can be determined and stated in the tables in section 4.2.

CHAPTER 4

RESULT AND DISCUSSION

4.1 Mode Shapes and Total Response for Lower Beam

Based on the matrix form of Equation (71), and using value of 5Hz, 10 Hz, 15 Hz, 20 Hz, 25 Hz and 30 Hz, by solving using inverse matrix method, all constant values of C_1 , C_2 , C_3 and C_4 for the lower beam can be determined and stated in the table below.

Table 4.1: Lower Beam's Value of C_1 , C_2 , C_3 and C_4 at 5 Hz

F = 5 Hz						
T(t) = sec	ω_f	β	C_1	C_2	C_3	C_4
100	31.42	1.976328	-0.01031	0.001136	0.010223	-0.00114
200	31.42	1.976328	-0.01893	0.002086	0.018772	-0.00209
300	31.42	1.976328	-0.02445	0.002695	0.02425	-0.00269
400	31.42	1.976328	-0.02597	0.002863	0.025759	-0.00286
500	31.42	1.976328	-0.02324	0.002562	0.023053	-0.00256
600	31.42	1.976328	-0.01671	0.001842	0.016574	-0.00184
700	31.42	1.976328	-0.00744	0.00082	0.007383	-0.00082
800	31.42	1.976328	0.003041	-0.00034	-0.00302	0.000335
900	31.42	1.976328	0.013028	-0.00144	-0.01292	0.001436

Table 4.2: Lower Beam's Value of C_1 , C_2 , C_3 and C_4 at 10 Hz

F = 10 Hz						
T(t) = sec	ω_f	β	C_1	C_2	C_3	C_4
100	62.84	2.79495	-0.00672	0.001043	0.00661	-0.00104
200	62.84	2.79495	-0.00922	0.001431	0.00907	-0.00143
300	62.84	2.79495	-0.00593	0.000921	0.005836	-0.00092
400	62.84	2.79495	0.00108	-0.00017	-0.00106	0.000168
500	62.84	2.79495	0.007413	-0.00115	-0.00729	0.001151
600	62.84	2.79495	0.009093	-0.00141	-0.00895	0.001412
700	62.84	2.79495	0.005064	-0.00079	-0.00498	0.000786

800	62.84	2.79495	-0.00214	0.000333	0.00211	-0.00033
900	62.84	2.79495	-0.00801	0.001243	0.007877	-0.00124

Table 4.3: Lower Beam's Value of C_1 , C_2 , C_3 and C_4 at 15 Hz

F = 15 Hz						
T(t) = sec	ω_f	β	C_1	C_2	C_3	C_4
100	94.26	3.4231	-0.00474	0.000898	0.004629	-0.0009
200	94.26	3.4231	-0.00324	0.000614	0.003163	-0.00061
300	94.26	3.4231	0.002528	-0.00048	-0.00247	0.000479
400	94.26	3.4231	0.00497	-0.00094	-0.00485	0.000941
500	94.26	3.4231	0.000869	-0.00016	-0.00085	0.000165
600	94.26	3.4231	-0.00438	0.000829	0.00427	-0.00083
700	94.26	3.4231	-0.00386	0.000731	0.003766	-0.00073
800	94.26	3.4231	0.001738	-0.00033	-0.0017	0.000329
900	94.26	3.4231	0.005047	-0.00096	-0.00493	0.000956

Table 4.4: Lower Beam's Value of C_1 , C_2 , C_3 and C_4 at 20 Hz

F = 20 Hz						
T(t) = sec	ω_f	β	C_1	C_2	C_3	C_4
100	125.68	3.952656	-0.00329	0.000716	0.00318	-0.00072
200	125.68	3.952656	0.000385	-8.4E-05	-0.00037	8.38E-05
300	125.68	3.952656	0.003241	-0.00071	-0.00314	0.000706
400	125.68	3.952656	-0.00076	0.000166	0.00074	-0.00017
500	125.68	3.952656	-0.00315	0.000686	0.00305	-0.00069
600	125.68	3.952656	0.001133	-0.00025	-0.0011	0.000247
700	125.68	3.952656	0.003019	-0.00066	-0.00292	0.000657
800	125.68	3.952656	-0.00149	0.000324	0.001439	-0.00032
900	125.68	3.952656	-0.00284	0.00062	0.002753	-0.00062

Table 4.5: Lower Beam's Value of C_1 , C_2 , C_3 and C_4 at 25 Hz

F = 25 Hz						
T(t) = sec	ω_f	β	C_1	C_2	C_3	C_4
100	157.1	4.419203	-0.00211	0.000512	0.002028	-0.00051
200	157.1	4.419203	0.001898	-0.00046	-0.00182	0.00046
300	157.1	4.419203	0.000407	-9.9E-05	-0.00039	9.87E-05
400	157.1	4.419203	-0.00226	0.000549	0.002173	-0.00055
500	157.1	4.419203	0.001627	-0.00039	-0.00156	0.000395
600	157.1	4.419203	0.000802	-0.00019	-0.00077	0.000194
700	157.1	4.419203	-0.00235	0.000569	0.002254	-0.00057
800	157.1	4.419203	0.001308	-0.00032	-0.00126	0.000317
900	157.1	4.419203	0.001173	-0.00028	-0.00113	0.000284

Table 4.6: Lower Beam's Value of C_1 , C_2 , C_3 and C_4 at 30 Hz

F = 30 Hz						
T(t) = sec	ω_f	β	C_1	C_2	C_3	C_4
100	188.52	4.840995	-0.00116	0.000307	0.001105	-0.00031
200	188.52	4.840995	0.001778	-0.00047	-0.00169	0.000471
300	188.52	4.840995	-0.00157	0.000414	0.001491	-0.00041
400	188.52	4.840995	0.000622	-0.00016	-0.00059	0.000165
500	188.52	4.840995	0.000612	-0.00016	-0.00058	0.000162
600	188.52	4.840995	-0.00156	0.000413	0.001486	-0.00041
700	188.52	4.840995	0.00178	-0.00047	-0.00169	0.000471
800	188.52	4.840995	-0.00117	0.000309	0.001112	-0.00031
900	188.52	4.840995	1E-05	-2.7E-06	-9.6E-06	2.66E-06

Based on the value of C_1 , C_2 , C_3 and C_4 , in Tables (4.1), (4.2), (4.3), (4.4), (4.5), and (4.6), we can produce the mode shapes and response of the micro UAV's lower beam structure with respect to the respective frequencies.

Frequency, F = 5 Hz

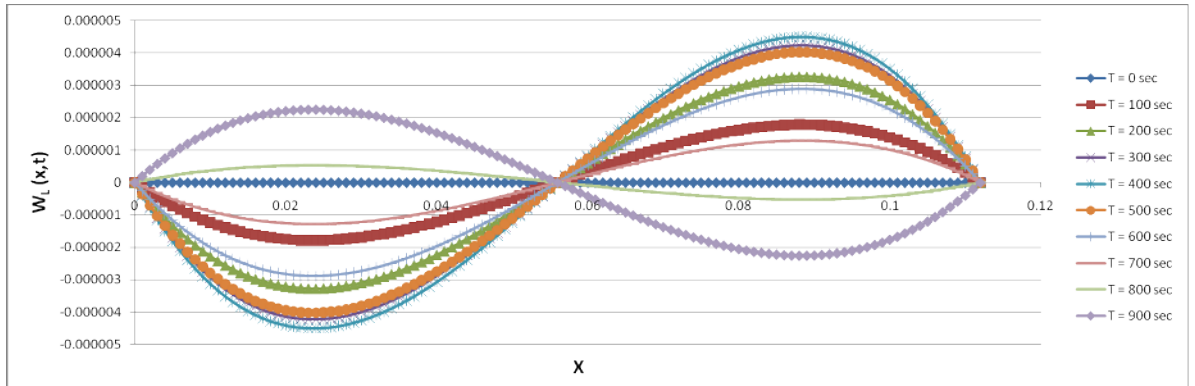


Figure 4.1: Response of the Lower Beam at 5 Hz

Applying frequency, $F = 5$ Hz to both fans at $x = 0.005$ m and $x = 0.107$ m, the values of C_1 , C_2 , C_3 and C_4 were figured out as stated in Table (4.1). Using the value of C , applying time, T , from 0 second, multiply 9 times with 100, until 900 seconds into the mathematical model, the shape and response of the lower beam was as in the Figure 4.1.

Frequency, $F = 10$ Hz

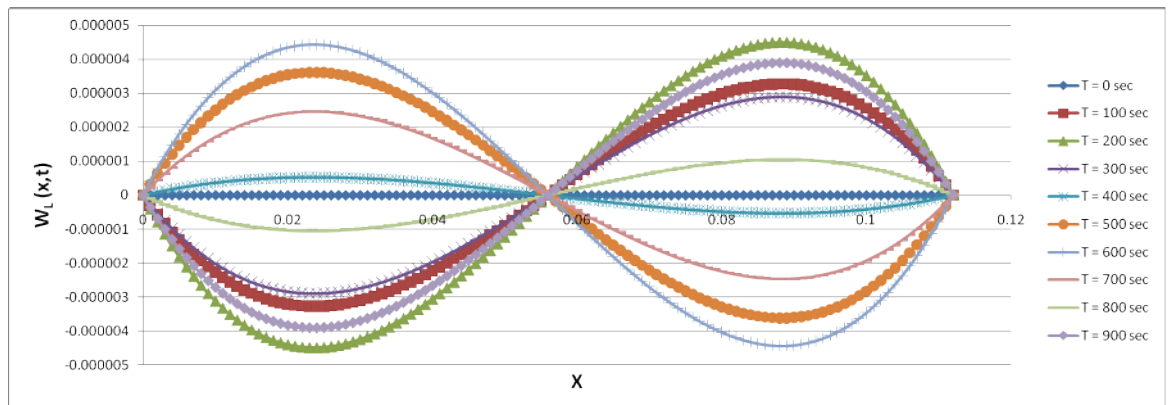


Figure 4.2: Response of the Lower Beam at 10 Hz

Applying frequency, $F = 10$ Hz to both fans at $x = 0.005$ m and $x = 0.107$ m, the values of C_1 , C_2 , C_3 and C_4 were figured out as stated in Table (4.2). Using the value of C , applying time, T , from 0 second, multiply 9 times with 100, until 900 seconds into the mathematical model, the shape and response of the lower beam was as in the Figure 4.2.

Frequency, $F = 15$ Hz

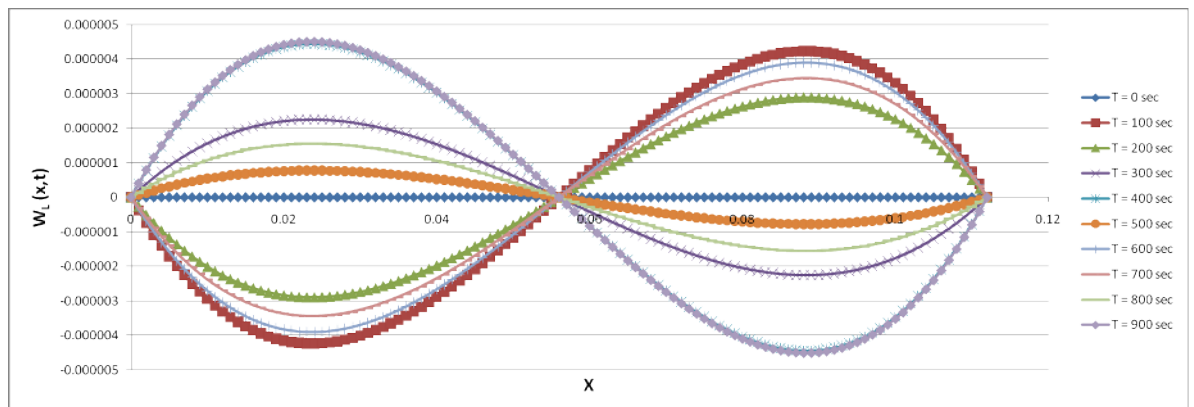


Figure 4.3: Response of the Lower Beam at 15 Hz

Applying frequency, $F = 15$ Hz to both fans at $x = 0.005$ m and $x = 0.107$ m, the values of C_1 , C_2 , C_3 and C_4 were figured out as stated in Table (4.3). Using the value of C , applying time, T , from 0 second, multiply 9 times with 100, until 900 seconds into the mathematical model, the shape and response of the lower beam was as in the Figure 4.3.

Frequency, $F = 20$ Hz

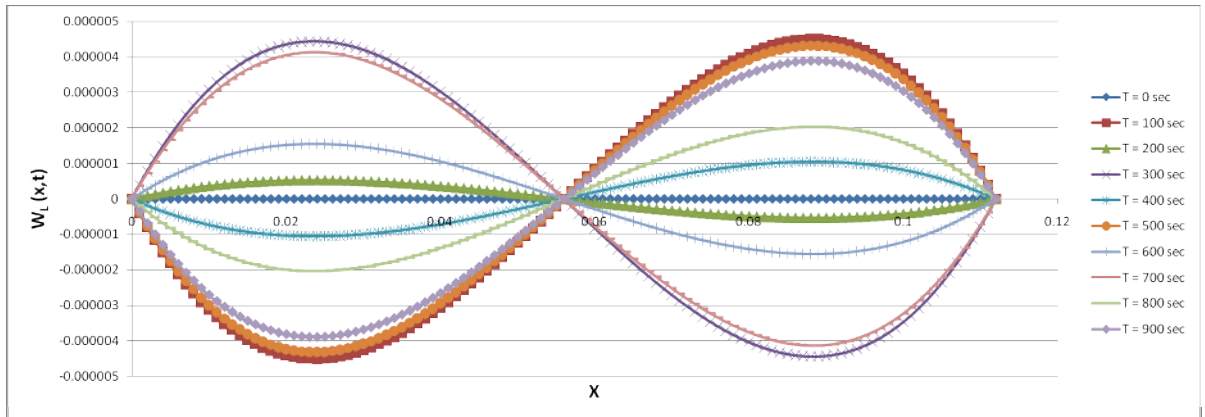


Figure 4.4: Response of the Lower Beam at 20 Hz

Applying frequency, $F = 20$ Hz to both fans at $x = 0.005$ m and $x = 0.107$ m, the values of C_1 , C_2 , C_3 and C_4 were figured out as stated in Table (4.4). Using the value of C , applying time, T , from 0 second, multiply 9 times with 100, until 900 seconds into the mathematical model, the shape and response of the lower beam was as in the Figure 4.4.

Frequency, $F = 25$ Hz

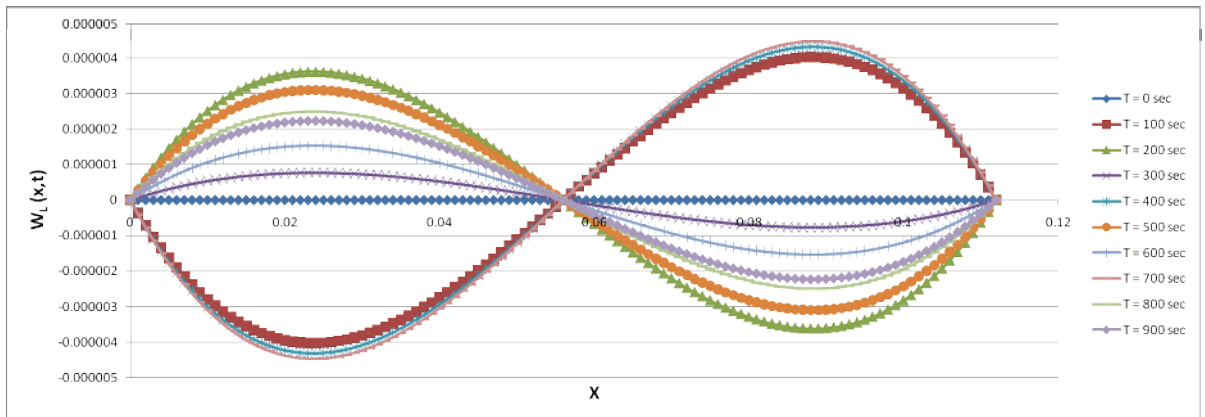


Figure 4.5: Response of the Lower Beam at 25 Hz

Applying frequency, $F = 25$ Hz to both fans at $x = 0.005$ m and $x = 0.107$ m, the values of C_1 , C_2 , C_3 and C_4 were figured out as stated in Table (4.5). Using the value of C , applying time, T , from 0 second, multiply 9 times with 100, until 900 seconds into the mathematical model, the shape and response of the lower beam was as in the Figure 4.5.

Frequency, $F = 30$ Hz

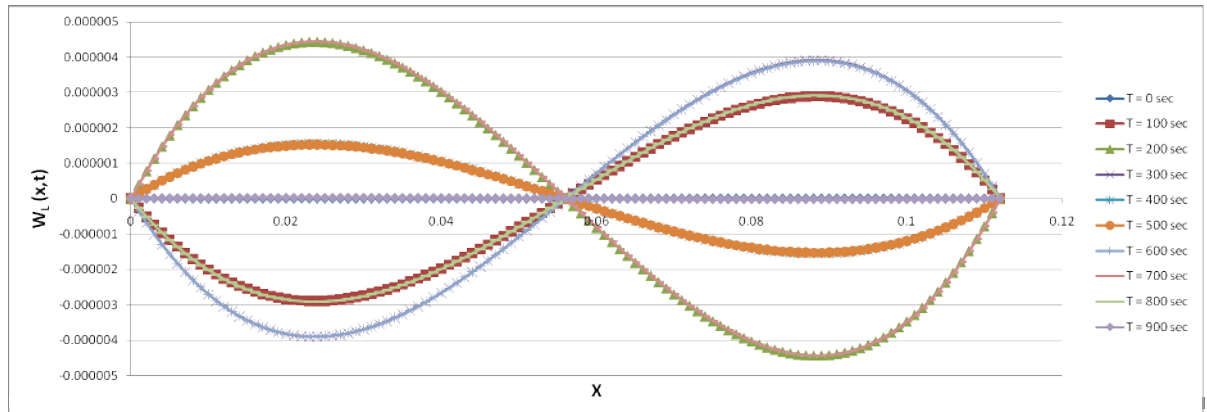


Figure 4.6: Response of the Lower Beam at 30 Hz

Applying frequency, $F = 30$ Hz to both fans at $x = 0.005$ m and $x = 0.107$ m, the values of C_1 , C_2 , C_3 and C_4 were figured out as stated in Table (4.6). Using the value of C , applying time, T , from 0 second, multiply 9 times with 100, until 900 seconds into the mathematical model, the shape and response of the lower beam was as in the Figure 4.6.

4.2 Mode Shapes and Total Response for Upper Beam

Based on the matrix form of Equation (83), and using value of 5Hz, 10 Hz, 15 Hz, 20 Hz, 25 Hz and 30 Hz, by solving using inverse matrix method, all constant values of C_1 , C_2 , C_3 , and C_4 for the upper beam can be determined and stated in the table below.

Table 4.7: Upper Beam's Value of C_1 , C_2 , C_3 and C_4 at 5 Hz

F = 5 Hz						
T(t) = sec	ω_f	β	C_1	C_2	C_3	C_4
100	31.42	1.874909	-0.01203	0.00062	0.012011	-0.00062
200	31.42	1.874909	-0.0221	0.001138	0.022057	-0.00114
300	31.42	1.874909	-0.02854	0.00147	0.028493	-0.00147
400	31.42	1.874909	-0.03032	0.001562	0.030266	-0.00156
500	31.42	1.874909	-0.02713	0.001398	0.027086	-0.0014
600	31.42	1.874909	-0.01951	0.001005	0.019474	-0.001
700	31.42	1.874909	-0.00869	0.000448	0.008674	-0.00045
800	31.42	1.874909	0.003551	-0.00018	-0.00354	0.000183
900	31.42	1.874909	0.01521	-0.00078	-0.01518	0.000784

Table 4.8: Upper Beam's Value of C_1 , C_2 , C_3 and C_4 at 10 Hz

F = 10 Hz						
T(t) = sec	ω_f	β	C_1	C_2	C_3	C_4
100	62.84	2.651522	-0.00782	0.000569	0.007791	-0.00057
200	62.84	2.651522	-0.01073	0.000781	0.010691	-0.00078
300	62.84	2.651522	-0.0069	0.000502	0.006879	-0.0005
400	62.84	2.651522	0.001257	-9.1E-05	-0.00125	9.15E-05
500	62.84	2.651522	0.008628	-0.00063	-0.0086	0.000628
600	62.84	2.651522	0.010582	-0.00077	-0.01054	0.00077
700	62.84	2.651522	0.005893	-0.00043	-0.00587	0.000429
800	62.84	2.651522	-0.0025	0.000182	0.002487	-0.00018
900	62.84	2.651522	-0.00932	0.000678	0.009285	-0.00068

Table 4.9: Upper Beam's Value of C_1 , C_2 , C_3 and C_4 at 15 Hz

F = 15 Hz						
T(t) = sec	ω_f	β	C_1	C_2	C_3	C_4
100	94.26	3.247438	-0.0055	0.00049	0.005474	-0.00049
200	94.26	3.247438	-0.00376	0.000335	0.003741	-0.00033
300	94.26	3.247438	0.002932	-0.00026	-0.00292	0.000262
400	94.26	3.247438	0.005765	-0.00051	-0.00573	0.000513
500	94.26	3.247438	0.001008	-9E-05	-0.001	8.98E-05
600	94.26	3.247438	-0.00508	0.000452	0.005049	-0.00045
700	94.26	3.247438	-0.00448	0.000399	0.004454	-0.0004
800	94.26	3.247438	0.002016	-0.00018	-0.00201	0.00018
900	94.26	3.247438	0.005855	-0.00052	-0.00582	0.000522

Table 4.10: Upper Beam's Value of C_1 , C_2 , C_3 and C_4 at 20 Hz

F = 20 Hz						
T(t) = sec	ω_f	β	C_1	C_2	C_3	C_4
100	125.68	3.749818	-0.0038	0.00039	0.003773	-0.00039
200	125.68	3.749818	0.000445	-4.6E-05	-0.00044	4.57E-05
300	125.68	3.749818	0.003748	-0.00039	-0.00372	0.000385
400	125.68	3.749818	-0.00088	9.08E-05	0.000878	-9.1E-05
500	125.68	3.749818	-0.00364	0.000374	0.003619	-0.00037
600	125.68	3.749818	0.001311	-0.00013	-0.0013	0.000135
700	125.68	3.749818	0.003491	-0.00036	-0.00347	0.000359
800	125.68	3.749818	-0.00172	0.000177	0.001707	-0.00018
900	125.68	3.749818	-0.00329	0.000338	0.003266	-0.00034

Table 4.11: Upper Beam's Value of C_1 , C_2 , C_3 and C_4 at 25 Hz

F = 25 Hz						
T(t) = sec	ω_f	β	C_1	C_2	C_3	C_4
100	157.1	4.192424	-0.00244	0.00028	0.002414	-0.00028
200	157.1	4.192424	0.002188	-0.00025	-0.00217	0.000251
300	157.1	4.192424	0.000469	-5.4E-05	-0.00047	5.39E-05
400	157.1	4.192424	-0.00261	0.0003	0.002587	-0.0003
500	157.1	4.192424	0.001876	-0.00022	-0.00186	0.000215
600	157.1	4.192424	0.000924	-0.00011	-0.00092	0.000106
700	157.1	4.192424	-0.00271	0.000311	0.002683	-0.00031
800	157.1	4.192424	0.001507	-0.00017	-0.00149	0.000173
900	157.1	4.192424	0.001352	-0.00016	-0.00134	0.000155

Table 4.12: Upper Beam's Value of C_1 , C_2 , C_3 and C_4 at 30 Hz

F = 30 Hz						
T(t) = sec	ω_f	β	C_1	C_2	C_3	C_4
100	188.52	4.592571	-0.00133	0.000167	0.001319	-0.00017
200	188.52	4.592571	0.002044	-0.00026	-0.00202	0.000257
300	188.52	4.592571	-0.0018	0.000226	0.00178	-0.00023
400	188.52	4.592571	0.000715	-9E-05	-0.00071	8.98E-05
500	188.52	4.592571	0.000704	-8.8E-05	-0.0007	8.84E-05
600	188.52	4.592571	-0.00179	0.000225	0.001775	-0.00023
700	188.52	4.592571	0.002046	-0.00026	-0.00202	0.000257
800	188.52	4.592571	-0.00134	0.000169	0.001328	-0.00017
900	188.52	4.592571	1.15E-05	-1.4E-06	-1.1E-05	1.45E-06

Based on the value of C_1 , C_2 , C_3 and C_4 , in Tables (4.7), (4.8), (4.9), (4.10), (4.11), and (4.12), we can produce the mode shapes and response of the micro UAV's upper beam structure with respect to the respective frequencies.

Frequency, $F = 5$ Hz

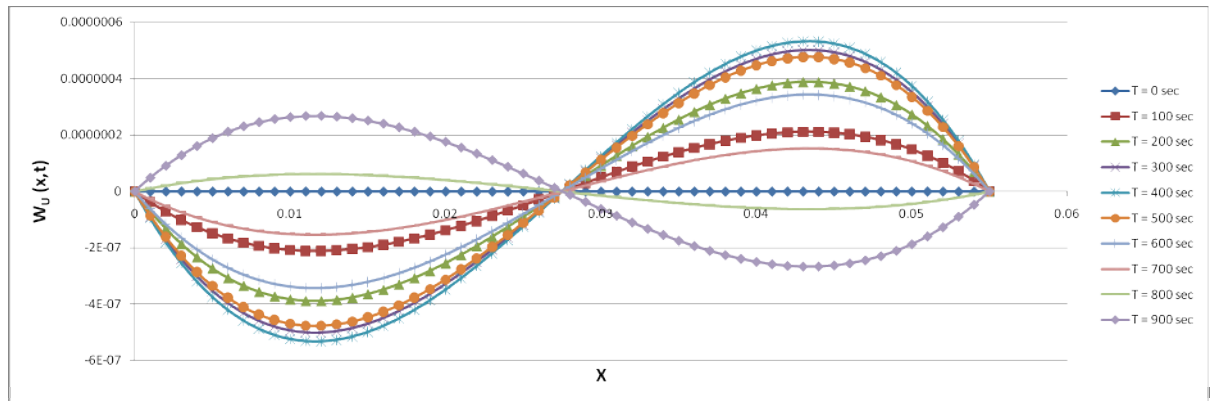


Figure 4.7: Response of the Upper Beam at 5 Hz

Applying frequency, $F = 5$ Hz to both fans at $x = 0.005$ m and $x = 0.05$ m, the values of C_1 , C_2 , C_3 and C_4 were figured out as stated in Table (4.7). Using the value of C , applying time, T , from 0 second, multiply 9 times with 100, until 900 seconds into the mathematical model, the shape and response of the upper beam was as in the Figure 4.7.

Frequency, $F = 10$ Hz

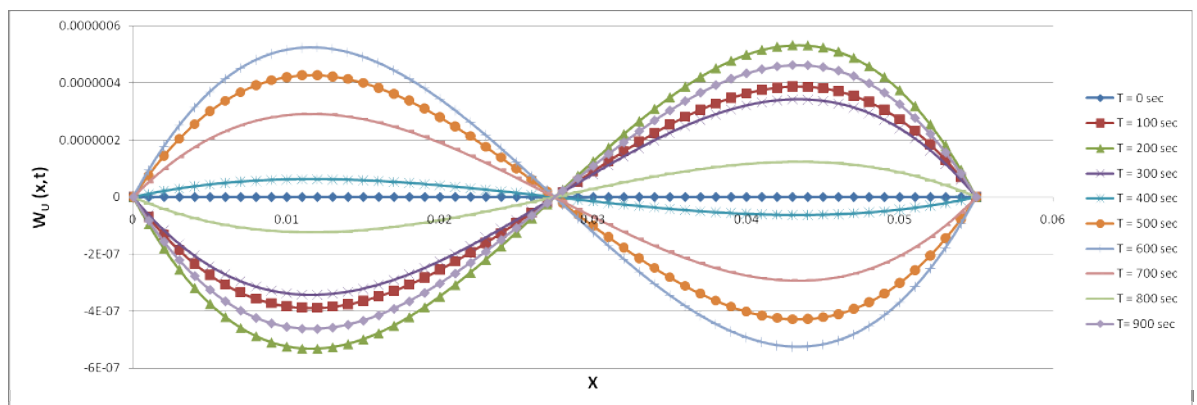


Figure 4.8: Response of the Upper Beam at 10 Hz

Applying frequency, $F = 10$ Hz to both fans at $x = 0.005$ m and $x = 0.05$ m, the values of C_1 , C_2 , C_3 and C_4 were figured out as stated in Table (4.8). Using the value of C , applying time, T , from 0 second, multiply 9 times with 100, until 900 seconds into the mathematical model, the shape and response of the upper beam was as in the Figure 4.8.

Frequency, $F = 15$ Hz

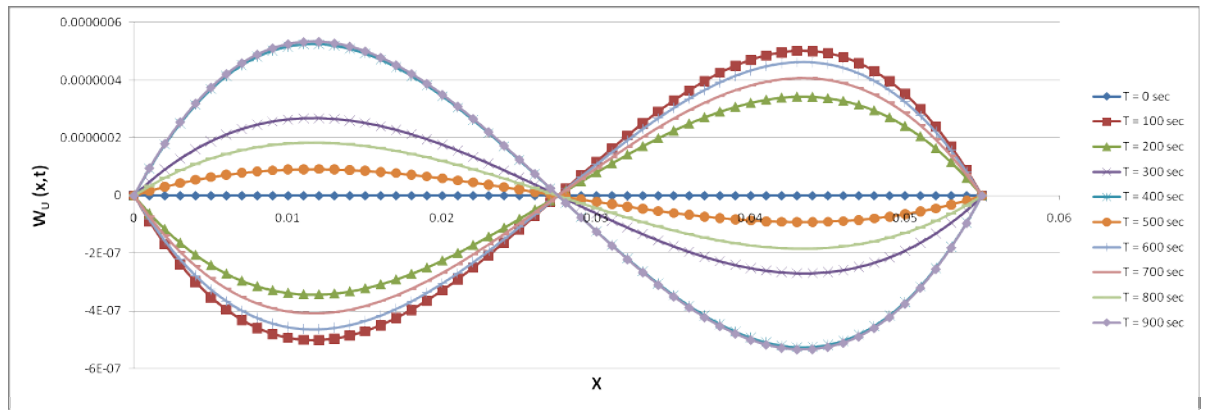


Figure 4.9: Response of the Upper Beam at 15 Hz

Applying frequency, $F = 15$ Hz to both fans at $x = 0.005$ m and $x = 0.05$ m, the values of C_1 , C_2 , C_3 and C_4 were figured out as stated in Table (4.9). Using the value of C , applying time, T , from 0 second, multiply 9 times with 100, until 900 seconds into the mathematical model, the shape and response of the upper beam was as in the Figure 4.9.

Frequency, $F = 20$ Hz

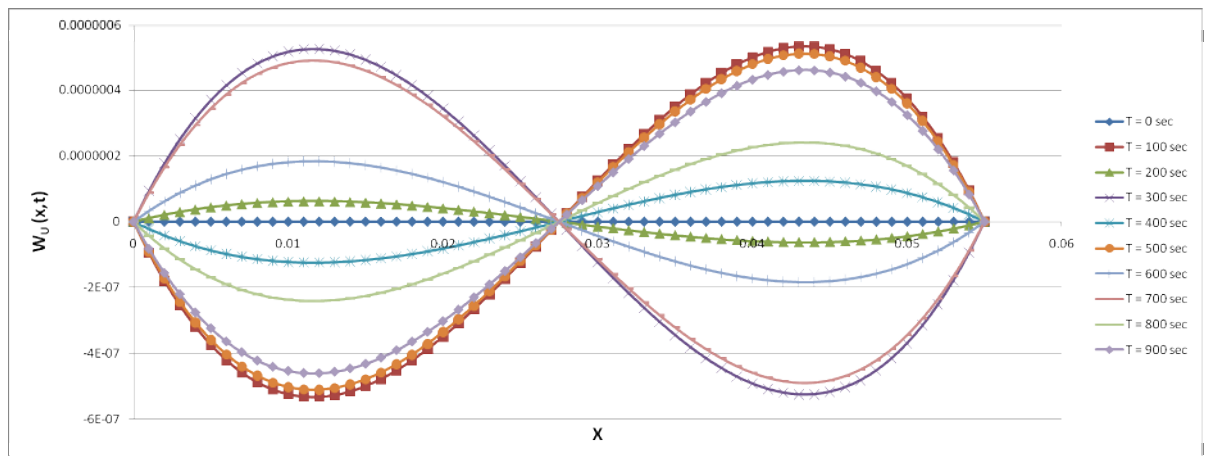


Figure 4.10: Response of the Upper Beam at 20 Hz

Applying frequency, $F = 20$ Hz to both fans at $x = 0.005$ m and $x = 0.05$ m, the values of C_1 , C_2 , C_3 and C_4 were figured out as stated in Table (4.10). Using the value of C , applying time, T , from 0 second, multiply 9 times with 100, until 900 seconds into the mathematical model, the shape and response of the upper beam was as in the Figure 4.10.

Frequency, $F = 25$ Hz

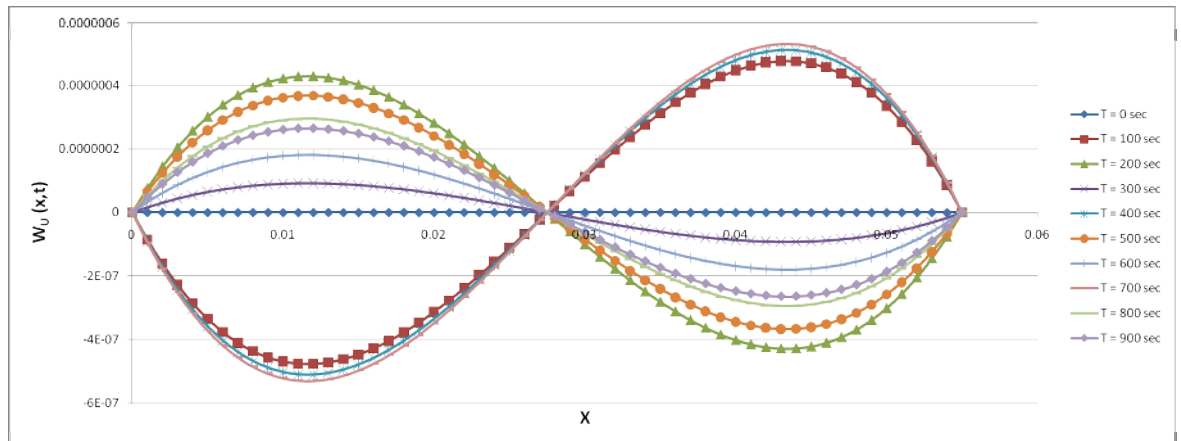


Figure 4.11: Response of the Upper Beam at 25 Hz

Applying frequency, $F = 25$ Hz to both fans at $x = 0.005$ m and $x = 0.107$ m, the values of C_1 , C_2 , C_3 and C_4 were figured out as stated in Table (4.11). Using the value of C , applying time, T , from 0 second, multiply 9 times with 100, until 900 seconds into the mathematical model, the shape and response of the upper beam was as in the Figure 4.11.

Frequency, $F = 30$ Hz

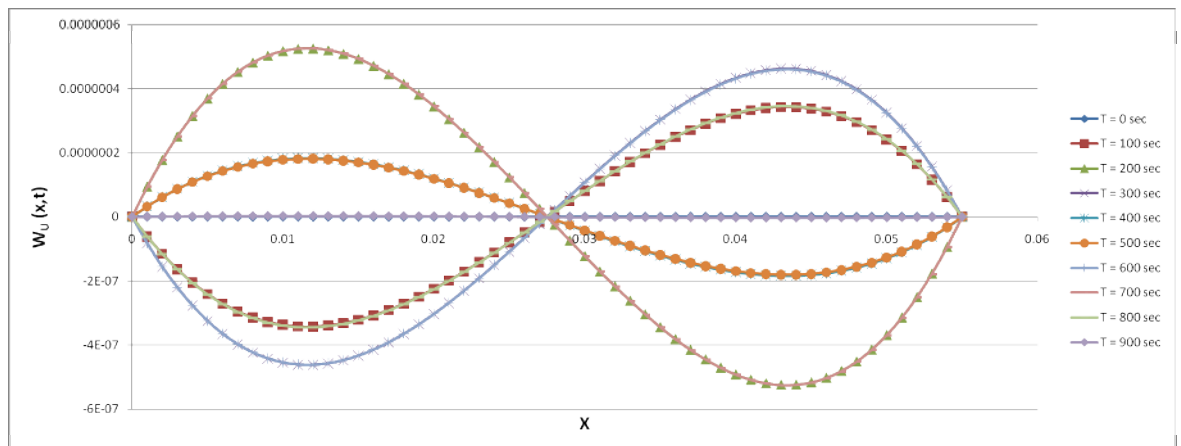


Figure 4.12: Response of the Upper Beam at 30 Hz

Applying frequency, $F = 30$ Hz to both fans at $x = 0.005$ m and $x = 0.05$ m, the values of C_1 , C_2 , C_3 and C_4 were figured out as stated in Table (4.12). Using the value of C , applying time, T , from 0 second, multiply 9 times with 100, until 900 seconds into the mathematical model, the shape and response of the upper beam was as in the Figure 4.12.

4.3 Discussion

This project is a comprehensive research study about harmonic response on the micro UAV's structure. The project is related to the study on the dynamic characteristics of the micro UAV's structure upon excitation by the wind load of the fans. Through out this project, the mode shapes and the responses of the micro UAV's structure for both lower and upper beam had been discovered. By substituting the respective values into the matrix form Equation (71), the value of constants C_1 , C_2 , C_3 , and C_4 for the lower beam had been calculated and being systematically arrange into Table (4.1), (4.2), (4.3), (4.4), (4.5), and (4.6), each of the table using different frequencies of fans. Using respective frequencies that had been decided before which are 5 Hz, 10 Hz, 15 Hz, 20 Hz, 25 Hz, and 30 Hz, and period of time between 0 seconds until 900 seconds which is 15 minutes, the responses of the lower beam had been shown in graphical type of chart with the exact length of the beam which is 0.11 meter. The calculated and generated mode shapes and the responses for the beam can be investigated from the Figure 4.1, 4.2, 4.3, 4.4, 4.5, and 4.6.

Same methodology with the lower beam, analysis also had been done onto the upper beam. Substituting respective values into the matrix form Equation 83, the value of constants C_1 , C_2 , C_3 , and C_4 for the upper beam had been calculated and being arrange into Table (4.7), (4.8), (4.9), (4.10), (4.11), and (4.12). Each of these tables were using different frequencies of fans, which were 5 Hz, 10 Hz, 15 Hz, 20 Hz, 25 Hz, and 30 Hz. Using respective frequencies that had been decided, and period of time between 0 seconds until 900 seconds (15 minutes), the response of the upper beam had shown in graphical chart with the exact length 0.055 meter. The completed generated mode shapes and the responses for the upper beam can be viewed from the Figure 4.7, 4.8, 4.9, 4.10, 4.11, and 4.12.

The mode shapes of both beams are following the general pattern of the mode shape for the beam with fixed end boundary condition. It means the mode shapes found out from the calculation process are valid since the pattern follow the expected mode shape pattern of a beam with respective boundary condition. The

figure below illustrated the general pattern of the mode shape with it respective t values.

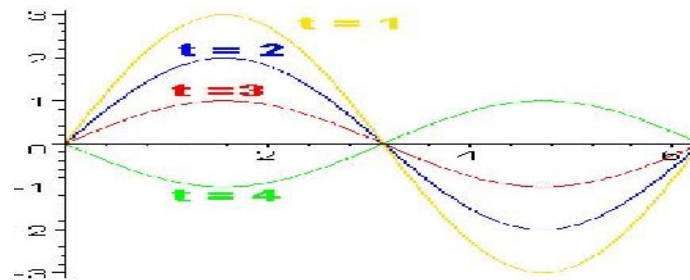


Figure 4.13: Mode Shape and Response of the Fixed End Beam with External Forces at $x = 1.5$ and $x = 4.5$ [7]

In this project, the value of ω_f for each fans are considered the same. In reality, the ω_f of the fans are supposedly different from each other due to the sources are from different equipments. So, for further studies, the ω_f need to be clarified to give better result in dynamic analysis as this project main focus is onto the structure's vibrations. As a part of methodology, simulation using software needs to be done to validate all the analysis that had been done. This is to compare either the analytical method chosen is correct to be used in dynamic analysis. Due to time constraint, simulation cannot be done but in future work, the analysis should be done to get a better result.

CHAPTER 5

CONCLUSION AND RECOMMENDATION

5.1 Conclusion

For this project, the methodology which is used in this project can support the objectives to find the three main relations in this project which are the natural frequency of Micro UAV structure, the respond and the mode shape under the influence of the fan speed. After reviewing the scope, time frame and the methodology of this project, it can be summarized that this project is a comprehensive research study on the dynamics analysis of the Micro UAV related to the design data, dynamics analysis and dynamics loading on the Micro UAV.

ABS had been considered for the structure material and dynamic analysis had been conducted to analyze the structure. Using Newtonian with analytical method, the mode shapes and the response the Micro UAV structure had been discovered. By substituting the value of constant C, and time T (form 0 until 900 seconds), the values found are stated in Tables (4.1) until (4.12). Using all the values and distance, x from 0 until 0.055 m for upper beam, and 0 until 112 m for lower beam, the shapes and the responses of the upper and lower beams are presented in Figure 4.1 until Figure 4.12. Based on the analytical method, the structure is achieved to sustain such dynamic loads applied on it. All the main objectives for this project were achieved.

5.2 Recommendation

For future work, all the analysis had to go through simulation using suitable software such as Ansys for validation purpose as the limitation of time in this project did not allow it to be done. Apart from that, the analysis also should be done in various methods and compare it to the current method used. It will give better result and more precise dynamic analysis.

REFERENCES

- [1] Singiresu S. Rao, Mechanical Vibration, University of Miami, *Prentice Hall*, 2005

- [2] Zahrul Fuadi and Zaidi Mohd. Ripin, Analysis of Design Parameter Effects on Vibration Modes of a Motorcycle Drum Brake and Brake Shoe Using the Finite Element Method, Universiti Sains Malaysia, *The Institution of Engineers, Malaysia (Vol 66, No 1)*, 2005

- [3] Q. S. Li, Free Longitudinal Vibration Analysis of Multi-step non-Uniform Bars Based on Piecewise Analytical Solutions, City University of Hong Kong, *Engineering Structures 22 1205-1215*, 1999

- [4] Mohd Anuar Bin Sulaiman, Structural Design of Micro Unmanned Aerial Vehicle (UAV), University of Technology PETRONAS, *Final Year Project Thesis*, 2009

- [5] R. C. Hibbeler, Mechanics of Materials, *Prentice Hall*, 2008

- [6] Magd Abdel Wahab, Dynamics and Vibration : An Introduction, *John Wiley & Sons, Ltd*, 2008

- [7] Benson H. Tongue, Principles of Vibration, University of California, *Oxford University Press*, 1996

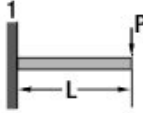
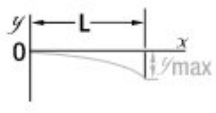
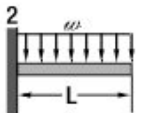
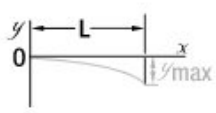
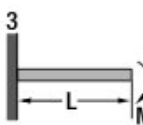
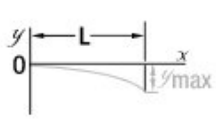
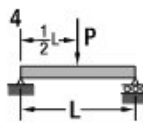
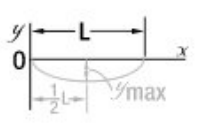
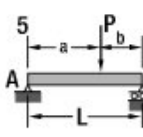
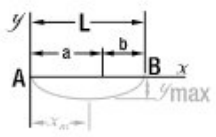
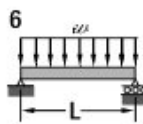
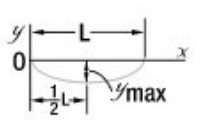
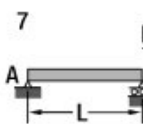
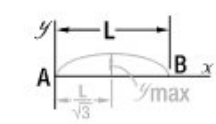
- [8] Andrew Dimarogonas, Vibration for Engineers, Washington University, *Prentice Hall*, 1996

- [9] William Weaver, Stephen P. Timoshenko & Donovan H. Young, Vibration Problems in Engineering, Stanford University, *John Wiley & Sons*, 1990

APPENDICES

APPENDIX A

Beam Deflections and Slope

Beam and Loading	Elastic Curve	Maximum Deflection	Slope at End	Equation of Elastic Curve
		$-\frac{PL^3}{3EI}$	$-\frac{PL^2}{2EI}$	$y = \frac{P}{6EI} (x^3 - 3Lx^2)$
		$-\frac{\omega L^4}{8EI}$	$-\frac{\omega L^3}{6EI}$	$y = -\frac{\omega}{24EI} (x^4 - 4Lx^3 + 6L^2x^2)$
		$-\frac{ML^2}{2EI}$	$-\frac{ML}{EI}$	$y = -\frac{M}{2EI} x^2$
		$-\frac{PL^3}{48EI}$	$+\frac{PL^2}{16EI}$	For $x \leq \frac{1}{2}L$: $y = \frac{P}{48EI} (4x^3 - 3L^2x)$
		For $a > b$: $\frac{Pb(L^2 - b^2)^{3/2}}{9\sqrt{3}EI}$ at $x_m = \frac{\sqrt{L^2 - b^2}}{3}$	$0_A = -\frac{Pb(L^2 - b^2)}{6EI}$ $0_B = +\frac{Pa(L^2 - a^2)}{6EI}$	For $x < a$: $y = \frac{Pb}{6EI} [x^3 - (L^2 - b^2)x]$ For $x = a$: $y = -\frac{pa^2b^2}{3EI}$
		$-\frac{5\omega L^4}{384EI}$	$+\frac{\omega L^3}{24EI}$	$y = -\frac{\omega}{24EI} (x^4 - 2Lx^3 + L^3x)$
		$-\frac{ML^2}{9\sqrt{3}EI}$	$0_A = +\frac{ML}{6EI}$ $0_B = -\frac{ML}{3EI}$	$y = -\frac{M}{6EI} (x^3 - L^2x)$

APPENDIX B

FINAL YEAR PROJECT I														
ACTION PLAN	SEMESTER JULY 2009													
	1	2	3	4	5	6	7	8	9	10	11	12	13	14
Introduction														
Problem Definition														
Project Planning														
Methodology Development														
Project Flow Chart														
Identification of tools														
Literature Review														
Study on the fundamental of continuous system														
Study on the mathematical approaches														
Mathematical Modelling														
Determine suitable mathematical method														
Develop mathematical model of micro UAV	FYP II							FYP II						
Develop equation of motion														
Develop total solution equation														
Determine the boundary condition														
Determine the total response														
Data Documentation														
Data collection														
Final Report														
FYP I														
Submission of Topic Proposal														
Submission of Preliminary Report														
Submission of Progress Report														
Seminar														
Submission of Interim Report														
Oral Presentation	During Study Week													

APPENDIX C

FINAL YEAR PROJECT II														
ACTION PLAN	SEMESTER JULY 2009													
	1	2	3	4	5	6	7	8	9	10	11	12	13	14
Introduction	FYP I						FYP I							
Problem Definition														
Project Planning														
Methodology Development	FYP I						FYP I							
Project Flow Chart														
Identification of tools														
Literature Review	FYP I						FYP I							
Study on the fundamental of continuous system														
Study on the mathematical approaches														
Mathematical Modelling														
Develop mathematical model of micro UAV														
Develop equation of motion														
Develop total solution equation														
Determine the boundary condition														
Determine the total response														
Data Documentation														
Data collection														
Final Report														
FYP II														
Submission of Progress Report I														
Submission of Progress Report II														
Seminar														
Poster Exhibition														
Submission of Dissertation Final Draft														
Oral Presentation	During Study Week													
Submission of Dissertation (Hard Bound)	7 Days After Oral Presentation													